U.PORTO
FEUP FACULDADE DE ENGENHARIA
UNIVERSIDADE DO PORTO
M 2023

DESIGN OPTIMIZATION OF A VEHICLE PLATFORM COMPONENT

BEATRIZ BARBOSA GONÇALVES
MASTER'S THESIS SUBMITED TO
FACULDADE DE ENGENHARIA DA UNIVERSIDADE DO PORTO

UNIVERSITY SUPERVISOR
PR. VITOR MARTINS-AUGUSTO

CEiiA SUPERVISOR
ENG. JOÃO ANUNCIAÇÃO

U.PORTO
FEUP FACULDADE DE ENGENHARIA
UNIVERSIDADE DO PORTO

CANDIDATO Beatriz Barbosa Gonçalves	*Código*

TÍTULO DESIGN OPTIMIZATION OF A VEHICLE PLATFORM COMPONENT

DATA	21 de Julho de 2023
LOCAL	Faculdade de Engenharia da Universidade do Porto – Sala F106 -14:30h

JÚRI	*Presidente*	DEMM/FEUP
	Arguente	DEM/FEUP
	Orientador	DEMM/FEUP

Resumo

A otimização topológica é uma abordagem promissora no projeto de engenharia, permitindo a criação de componentes únicos. Esta tese explora a função "Design Generativo" do Fusion 360, um software da Autodesk, como um método para otimizar, em tempo reduzido, componentes de um veículo ainda em desenvolvimento.

Os componentes selecionados foram uma junta de direção e um braço de direção de uma suspensão triângulo duplo. Devido à elevada complexidade do componente, houve secções dos componentes com um grau de otimização reduzido em comparado com outras, no entanto, para a junta de direção, foi possível atingir 30% de redução de massa, demonstrando os potenciais benefícios do software em estudo. No que diz respeito aos braços de direção, algumas simulações falharam em atingiram o fator de segurança mínimo exigido de 2, dentre a presença de deslocamentos percetíveis.

Este trabalho também enfatiza a influência de restrições e corpos de obstáculos nos resultados gerados. Com o aumento da complexidade, a qualidade de resultados foi comprometida, levantando dúvidas sobre a capacidade do solver em lidar com cenários de alta complexidade.

Este software destaca-se pela sua interface amigável e flexibilidade na incorporação de inputs. No entanto, a versão atual do Fusion falha em cumprir na totalidade as suas promessas quando confrontada com requisitos complexos.

KEYWORDS

Topological optimization, Fusion 360, Generative Design, Aluminum, Casting, Additive Manufacturing, Steering Knuckle, Control arm, Suspension, Simulation

ACKNOWLEDGMENTS

I would like to thank my supervisors, Professor Vitor Martins Augusto and Engineer João Anunciação, for their support, and guidance throughout the development of this work.

To all my family and friends, thank you for your support and continuous motivation through this five years journey.

TABLE OF CONTENTS

RESUMO III
KEYWORDS III
ACKNOWLEDGMENTS IV
TABLE OF CONTENTS V
1. INTRODUCTION 1
1.1. GENERATIVE DESIGN 1
1.2. TYPE OF SUSPENSIONS 2
1.3. STEERING KNUCKLE 4
1.4. CONTROL ARM 5
2. LITERATURE SURVEY 6
3. PLANNING 8
4. DEVELOPMENT 9
4.1. MANUFACTURING METHODS 10
4.2. MATERIAL SELECTION 11
4.3. GEOMETRY REQUIREMENTS 14
4.4. DEFINITION OF LOADS 16
5. SIMULATIONS 19
5.1. FUSION 360 GENERATIVE DESIGN 19
5.2. STEERING KNUCKLE 20
5.2.1. FIRST GEOMETRY 20
5.2.2. DESIGNS CREATED BY GENERATIVE DESIGN 26
5.2.3. DESIGNS CREATED BY SHEET METAL FUNCTION 39
5.3. CONTROL ARM 40
5.3.1. FIRST GEOMETRY 40
5.3.2. DESIGNS CREATED BY GENERATIVE DESIGN 42
6. RESULT ANALYZIS 47
6.1. STEERING KNUCKLE 49
6.2. CONTROL ARM 50
7. CONCLUSION 51
BIBLIOGRAPHY 52
APPENDIX 59

Figure 1 - Independent and non-independent suspension, retrieved from [3] 2
Figure 2 - Types of suspensions 4
Figure 3 - Evolution of used materials [24] 5
Figure 4 - Methodology 9
Figure 5 - Relation between unitary cost with complexity, on the left, and number of produced parts, on the right, for conventional and additive manufacturing [47,48] 10
Figure 6 - Materials Properties, Retrieved form [73] 13
Figure 7 - Steering system assembly 14
Figure 8 - Steering system detailed 14
Figure 9 - Component's initial geometry 15
Figure 10 - Non-Design space of each component 16
Figure 11 - Load Points 18
Figure 12 - Generative Design available inputs 19
Figure 13 - Component's alternative initial geometry 20
Figure 14 - Results Color Gradient 21
Figure 15 - Initial geometry - FoS simulation results 22
Figure 16 - Initial geometry - Displacement and Stress simulation results 23
Figure 17 - Simpler geometry - Displacement and Stress simulation results 24
Figure 18 - "Bulk" geometry - Displacement and Stress simulation results 25
Figure 19 - Simulations S1 - S6 26
Figure 20 - Lack of connection present in the generated results 27
Figure 21 - Simulations S7 - S9 27
Figure 22 - Geometry Correction 28
Figure 23 - Lower Control arm movement 28
Figure 24 - S10 28
Figure 25 - S10 results 29
Figure 26 - S11 30
Figure 27 - S12 31
Figure 28 - S13 32
Figure 29 - Simulations S14 - S17 33
Figure 30 - S14 - S17 solutions when there are several constraints 34
Figure 31 - S15 - S17 solutions when there is only one constraint 35
Figure 32 - S14 solutions when there is only one constraint 36
Figure 33 - S18 results for a new list of materials 37
Figure 34 - Steering Knuckle geometry created for sheet metal forming 39
Figure 35 - Results of the simulation of sheet metal model 40
Figure 36 - Control Arm's constraints for initial simulation 41
Figure 37- Results of the simulation on the initial geometry 42
Figure 38 - Constraints used during Control arm's simulations 42
Figure 39 - S1 (Control Arm), conditions on the left and result, on the right 43
Figure 40 - S2 (Control Arm) 43
Figure 41 - S3 (Control Arm) 44
Figure 42 - S4 and S5 (Control Arm) 44
Figure 43 - S4 and S5 example results 44
Figure 44 - S6 (Control Arm) 45
Figure 45 - S6 (Control Arm) results 45
Figure 46 - S7 (Control Arm) 46
Figure 47 - S7 (Control Arm) FWOB result 46
Figure 48 - S7 (Control Arm) PB result 46
Figure 49 - S7 (Control Arm) CURB results 47
Figure 50 - Die Casting Results 47
Figure 51 - Error Notices 48
Figure 52 - FoS Analysis 51
Figure 53 - Displacement Analysis 51

Table 1 - Materials Properties, Retrieved from [73] 13
Table 2 - Load Cases 1 applied to the Steering Knuckle 17
Table 3 - Load Cases 2 applied to the Steering Knuckle 17
Table 4 - Load Cases applied to the Control arm 17
Table 5 - First analysis results 21
Table 6 - Summary of all simulations 38
Table 7 - Simulation results 39
Table 8 - Simulation Results 41
Table 9 - Best results comparison – Steering Knuckle 49
Table 10 - Best results comparison – Control Arm 50

1. Introduction

The competition in the automotive industry is fierce and manufacturers strive to continuously achieve success. To accomplish this goal, companies employ various strategies to enhance their chances of success, investing heavily in research and development to create cutting-edge technologies. The focus is to create unique styles, performance capabilities, and groundbreaking features such as autonomous driving, electric propulsion among others, not only to attract new customers.

Cost efficiency is also a vital consideration as companies strive to provide competitive prices while maintaining high-quality standards. Through the implementation of CAD (Computer Aided Design), CAE (Computer Aided Engineering), and CAM (Computer Aided Manufacturing) it is possible to achieve cost efficiency. These tools enable the creation of reduced-cost components by simulating real-life situations, predicting the stress, displacement, among other factors that the components will experience over time. By utilizing these software, companies can effectively analyze the production process of components, identifying potential manufacturing defects, and, even predict the overall manufacturing cost.

It can be argued that continuous innovation, quality prioritization, branding investment, cost optimization, and filling costumers' expectations, are crucial factors to the endure the success of a company.

Currently, the process of generating and optimizing 3D models requires significant a amount of time and specialized software. This thesis was developed in collaboration with CEiiA utilizing Fusion 360's generative design as an innovative approach to optimize, in reduced time, chassis components for a car under development. This selection was due to the software's user-friendly approach and the ability to generate several results in a reduced timeframe. The chassis was selected since it plays a major role in the total cost, weight, ride, and handling of a car, and the geometry and properties each component has contribute to the safety and driving characteristics [1]. To summarize, the primary objective of this thesis is to create topologically optimized models of two chassis components, aiming to a weight reduction without compromising mechanical properties and safety of the vehicle.

1.1. Generative Design

Currently, there is a focus on achieving light-weight components, therefore, in the development period of a component, there is a necessity to submit the components to a topological optimization operation or, use specific software that generates results according to the added data.

Topological optimization corresponds to an optimization of the material distribution by removing unnecessary material and redistributing it where it meets desired performance objectives. With the reorganization of the material, it is possible to verify mass reduction, verifying a reduction in fuel consumption, a contribution to a more sustainable industry, creation of new, and previously impossible to obtain geometries, improves aerodynamic aspects, use of new materials, that could contribute with better

mechanical attributes. Topological optimization is a crucial role in this industry since it is a huge factor in the creation of a revolutionary design of lightweight and high-performance components. The components selected for this study are part of the chassis since it takes between 25 to 30% of the vehicles' weight [2].

Choosing the correct software for topological optimization, or generative design, will create the best results for each indicated load case, considering all the physical and mechanical properties of the materials involved and boundary conditions and using sophisticated algorithms and computational tools.

1.2. Type of suspensions

When planning any type of vehicle, it is mandatory to follow a list of requirements that will influence factors such as safety, stability, handling under all driving conditions, vehicle behavior, comfort, while keeping the lightweight, low cost, manufacturing, ease repair, recyclability. Each manufacture will choose which requirements are more relevant to their market segment since it is not possible or necessary for any vehicle to be the best in all the categories [1].

In an **independent suspension**, the installation is individual on each wheel, resulting in a more comfortable, safer, and controlled ride, at high speeds and tight corners. This means any bumping, on one wheel, will be eliminated or reduced, not affecting the others. McPherson, Double Wishbone, and multi-link are examples of independent suspensions [3].

In **non-independent suspensions**, the behavior of one wheel will affect the rest of the vehicle, affecting safety and stability [3].

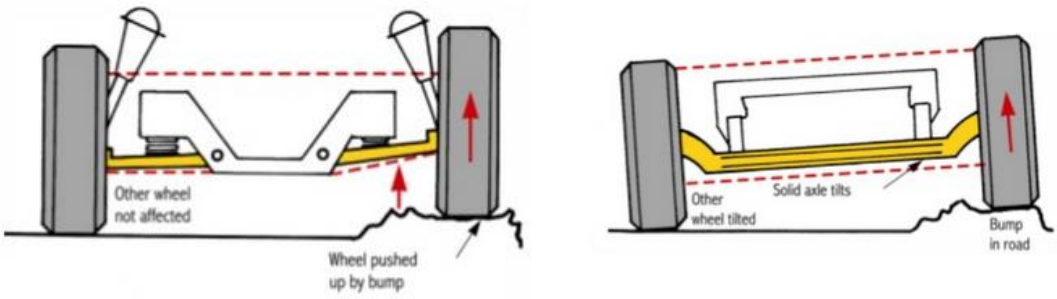


Figure 1 - Independent and non-independent suspension, retrieved from [3]

A **MacPherson** is one of the most used models since it combines extreme comfort and control with a simple design, reduced manufacturing costs, wide availability, and easy manipulation upon requirements from the vehicle or the driving situation. Regarding the geometry, it has a damper connected to the upper region, while the control arm is attached to the lower section. This assembly allows the chassis and wheel to move in unison. However, it is neither the greatest tire grip in turns nor the highest capacity for receiving loads [3, 8].

The **double-wishbone** suspension is one of the most sophisticated models and is the most efficient at minimizing the effect of road irregularities and has the best packaging due to the low profile. The suspension's name is derived from the resemblance between both A-shaped arms present in the component with wishbones. This arrangement increases, even at high speeds, the control, and comfort, being suitable for fast cornering. These attributes allow it and its modified versions to be included in luxury, sport, and race cars. Although they are durable and it is expected a low number of repairs or replacements, when needed, this process requires a skilled mechanic, time, and money due to the high complexity and weight of the structure [8].

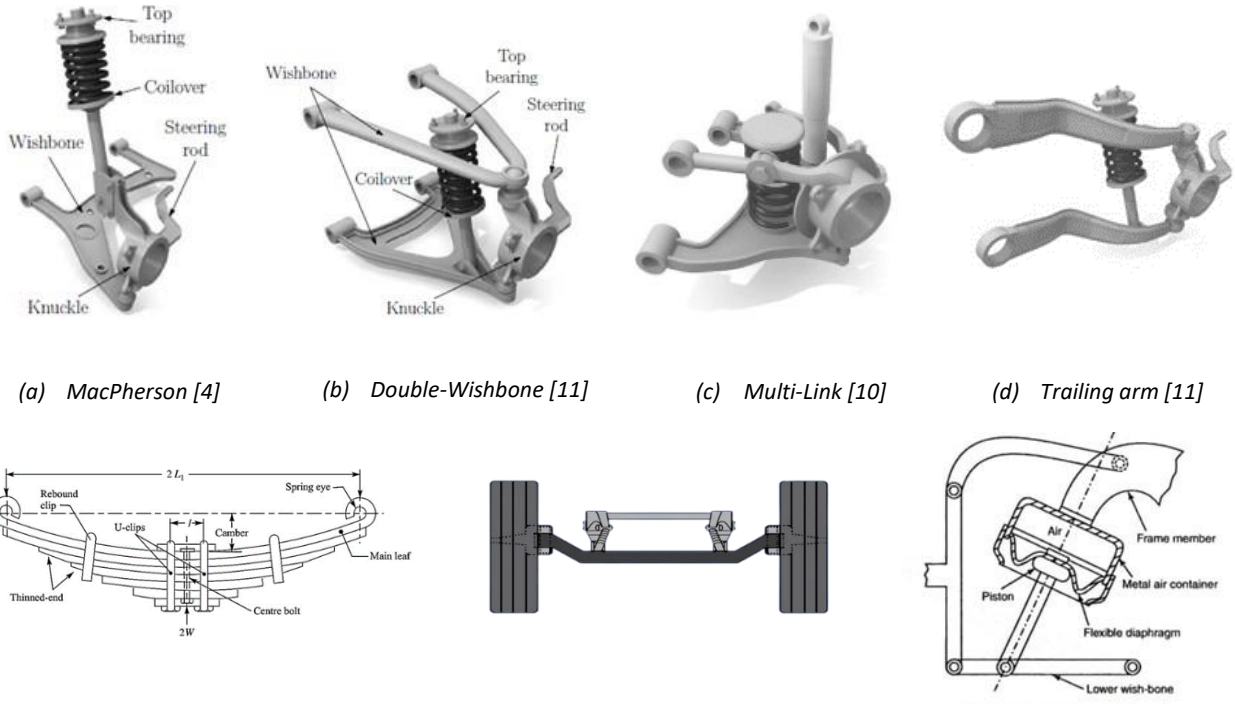
A **multi-link** suspension has a complicated construction since it has several links, held together by joints, between the chassis and the steering knuckle. The direction of the movements influences the position and direction of the links on each wheel. It is able to balance most of the shocks they suffer, guaranteeing a high-quality tight grip on quick turns, being enticing to off-road vehicles, specifically, the rear wheels. Generally, they are found on high-end vehicles, since it is an expensive type of suspension, and the maintenance has a high cost [9].

Despite the previously mentioned suspensions having the damper shaped as coils, the **rigid/leaf suspensions** are composed of leaf springs, bundles of spring materials, mostly steel, with the capacity to flex when pressed by the vehicle's axle. This geometry is strong enough to hold high loads and can easily reduce the bumps that a vehicle encounters, being a great fit with commercial use vehicles, however, they are not ideal for comfort neither high speed nor fast turning [10].

The **beam axle suspension, or rigid axle suspension**, has a perpendicular axle attached, with a wheel spindle, to the wheels, using either leaf or coiled springs. The main characteristic is the sturdiness and the capacity to hold considerable weight, being commonly used in vehicles that carry significant amounts of weight or off-roaders, not being suitable for higher speeds or sharp turns, having an increased risk of rollover when submitted to those. The simple configuration is an advantage in fixing or replacing the component [11].

Air suspension or **air springs** use air instead of coils and dampers, being inflated or deflated, aided by an air compressor, to modify the vehicle's height. It is one of the most comfortable and load-bearing suspensions available, being mostly applied in high-end luxury and sports vehicles, due to the complicated construction and high price, and, the load bearing, allows the application into buses or other types of automobiles. They are also easily adaptable, and, with proper equipment, the comfort of the ride is amplified, since they can adjust to any preference, such as passenger, loads, or height [12].

The **trailing arm suspension** is mostly used on the rear of the vehicle, ideally on a lighter vehicle, such as a motorcycle, since upon high loads, the arms tend to bend, unabling the vehicle. It is characterized for having a steel arm between the chassis and the rear axle, as well as a damper. Ideally, they are applied in motorcycles, since, upon high loads, the arm tends to bend, unabling the vehicle [11, 12].



(a) MacPherson [4] *(b) Double-Wishbone [11]* *(c) Multi-Link [10]* *(d) Trailing arm [11]*

(e) Rigid/Leaf [10] *(f) Beam Axle [11]* *(g) Air Springs [11]*

Figure 2 - Types of suspensions

1.3. Steering Knuckle

A knuckle has the primary function of holding the weight of the vehicle and directing the forces from the wheel to the suspension system. Alongside this, they also hold the brake caliper, and convert linear motion of the tie rod to angular motion of the stub axle. Additionally, depending on which wheel they are attached to, some of them are also in steering applications [1, 13 – 23].

Upon steering the steering knuckle is subjected to a torsional load, due to half of it being exposed to tensile load and, the other half, to compressive loads, being a requirement the capacity to support loads and torque induced by bumping, braking, and acceleration. All these loads and the function of the component urge regular and complete analysis by the design teams since with any type of damage or eventual fracture, the vehicle is unable from operating [1, 27 – 30].

To maximize a knuckle's potential, it should be strong, inflexible, and as light as possible. The minimization of the mass holds innumerous advantages, it reduces fuel consumption, and, more importantly, it improves efficiency since inertia is lower, and, although the power remains high, there is less vibration.

The first steering wheels date back at the beginning of the 19th century. It is reported that in 1970 many steering knuckles were being produced as ductile iron castings and spheroidal graphite (SGI). Between 1990 and 2000, those materials were mainly applied to trucks, while automobiles also opted for cast aluminum and compact graphite iron,

CGI. Recently, with the new goals of reducing the weight of the vehicle, there was a significant growth on the use of cast aluminum knuckles, manufactured by semisolid molding process and conventional permanent molds, Figure 3. A small amount of knuckles can also be produced by CGI due to the lighter weight and lower cost [1, 24, 25].

Component	Pre 1990		1990–2000		2005+	
	T	A	T	A	T	A
Subframes	fabricated steel		steel fabs aluminum fabs, cast Al		steel, HSLA steel, cast Al	
Springs	steel		Steel		steel, HSLA steel, reinf plas	
Control arms	fab steel	SGI	fab steel	cast Al (50%)	steel, HSLA steel, cast Al	
Knuckles	SGI		SGI	CGI, SGI, cast Al	Cast Al	
Shocks	fabricated steel		fabricated steel		fab steel	Ti, steel
Wheels	steel	cast Al	cast Al, steel	cast Al, steel	cast Al, steel	cast Al, Mg
Brake rotors	GCI		GCI		GCI	GCI MMC Al
Brake drums	GCI		GCI	GCI, MMC Al	GCI	GCI, MMC Al
Calipers	SGI		SGI	GCI, Al, MMC Al	SGI	Al, MMC Al

SGI, spheroidal graphite or ductile cast iron; CGI , compacted graphite cast iron; GCI, gray cast iron; reinforced plastic, composite of polymer with fiber glass; MMC Al, composite of aluminum with SiC particles; SSM Al, semisolid molded or cast aluminum; fab steel, fabricated, usually by welding steel tubing; HSLA steel, high-strength low-alloy steel.

Figure 3 - Evolution of used materials [24]

According to [31, 32], forging takes up most of the production of steering knuckles, however, there are some limitations, for example, low efficiency, a quality that is rarely satisfactory, and a long processing time. For the past couple of years and, it is predicted for the near future, casting has had a 5.8% growth. This process is more cost-effective for mass production and has higher freedom for geometries than the previous one, but it can also have defects such as cracks, porosity, drawbacks, and weak finishing, among others.

Both forging and casting processes require a machining process to guarantee dimensional accuracy [27]. There are different types of castings to choose from, such as Counter Pressure Casting (CPCP), an evolution of low-pressure die-casting that is getting more relevant and produces millions of automotive safety-critical castings every year. This process yields strengths between 85 and 90%, similar to low-pressure casting, and the properties are usually better than sand and gravity permanent molds and low-pressure castings due to the filling and feeding characteristics, mold/casting heat transfer efficiency, melt cleanliness, and low levels of gas porosity. Vacuum riserless/pressure riserless casting (VRC/PRC) is also an option, the mechanical properties are similar to squeeze castings [25].

1.4. Control arm

Control arms are mechanically impressive parts since they are the connection between the front wheels and the vehicle. Although their appearance is simplistic, they have a vital role in overall stability and drivability [32, 33].

They can be A, L, or wishbone-shaped, depending on the suspension geometry, and are attached by bolts and bushings to a hinge. The presence of a ball joint allows the wheel to move smoothly in all directions, allowing the wheels to turn while in motion. Being subjected to a great deal of stress and impact, it has a limited lifespan, depending mainly on the type of drive.

Nowadays, they are composed of stamped steel, cast iron for higher strength and sturdiness, and cast aluminum for light-weight purposes. Initially, control arms were commonly made from stamped steel since it was cheap, fast, and easy. It is used to hold coil springs in place on full-framed cars and provide attachment points for shocks and sway bars. It had the big disadvantage of suffering from rust, which is nearly guaranteed when they are stamped in a wet environment. There is a point where the grade of rust is so high that it becomes almost a challenge to replace the bushing and ball joints without damaging the control arm, however, the replacement is almost inexpensive, and replacing the entire assembly implies less labor than replacing each component individually [32, 33].

Cast iron started being implanted into modern vehicles, such as trucks and SUV's. The front suspensions are usually wishbone-shaped, being extremely strong and able to withstand harsh environments better than the stamped steel control arms. Currently, with the aim of achieving lightweight components, there has been an evolution, and control arms have evolved to elaborate cast aluminum components, Figure 3, which are lighter and stronger than before and have lower corrosion, but because they are a soft metal, they bend and crack easier, meaning that it is easier to throw the alignment off [33].

2. Literature survey

By conducting a thorough literature review, this study aims to identify and analyze similar studies that have previously investigated these components. The survey will provide valuable insights into the current state of knowledge and the most commonly used software, geometries, load cases, materials, and manufacturing methods, among others.

Ultimately, the findings from this literature survey will contribute to a better understanding of both components and serve as a starting point for the development of this thesis.

[13] Mirzana I. et. al. (2018) tested different materials in the same application (Al alloy, grey cast iron, AISI 4340 (Structural steel), and magnesium alloy), identifying the structural steel as the material with the minimum deformation. After optimization, it was possible to verify a weight reduction of 6.163% and less 65% deformation than the initial model.

[15] Mirzana Deshpande, Aditya et. Al. (2020) focused on obtaining the minimum weight possible, choosing an aluminum alloy (6061 T6), achieving a final model weighting 0.6kg, having a reduction of 1.8 kg. The CAD model was prepared in Solid works 2016, and the load analysis were made in ANSYS Workbench 15.0.

[16] Harsha, J. S. (2016), also pursued an analysis between two materials, Al 6082 T6 and grey cast iron, they modeled in Solid Works and analyzed, in Ansys Workbench the conditions for bumping, cornering and braking a steering knuckle manufactured by using CNC machinery, realizing that the aluminum alloy, in these conditions, should be the one

to be chosen.

[17] Kamble, A. V. et. al. (2017) used CATIA V5 and HYPERMESH in the scope of reducing the weight of a mild steel, produced by forging and turning, knuckle, achieving a reduction of mass of 9.86%, of stress of 27.76% and displacement of 24.42%.

[18] Yadav, S. et. al. (2016) worked towards updating their model and materials used. With that scope, they used Creo (Pro-E) 2.0 and ANSYS WORKBENCH 15.0. The initial material was mild steel (yield strength 250 MPa) and weighted around 3.72 kg, the study allowed them to create a new steering knuckle, of Forged Steel EN47, with maximum yield strength of 650 MPa, and a mass reduction of 5.64%, obtaining 3.51 kg.

[19] Jeon, G. T. et. al. (2018) innovated and decided to adjust the composition of an aluminum alloy in order to obtain the desired properties. Therefore, they used a tailored additive casting (TAC) to successfully produce an alloy with an average tensile strength of 383 MPa, and elongation of 10.7 % on an alloy of Al 6061 using Zr, Zn, and Cu as minor elements. By producing by this method, there is no need for subsequent processing to remove excess material.

[20] Patil, G.B. et. al. (2016) focused on the weight reduction, obtained a model with 2.24 kg, corresponding to a 12.56% reduction on a steering knuckle adapted to a MacPherson suspension. The utilized softwares were CATIA V5, Hyper Mesh and Hyper-Works.

[34] Jhala, R. L. et al (2010) did a complete study to understand the impact of a few aspects on the final cost of the process, for example, attending to the changes in geometry or manufacturing processes. By changing the geometry, without altering the forging cost, there is a 9.4 % weight saving, and the stress levels, although higher in some points, are still lower than critical. They also came to the conclusion that by reducing machining time, the final cost, and waste will be lower, as well as some manufacturing processes may imply some additional costs and the overall performance may not justify the selection of the process.

[22] Triantafyllidis, G. K., et. al. (2009) evaluated the behavior of different irons to understand the one with the best fatigue performance. They realized that ductile iron had a better performance than other cast irons, however it is still lower than the fatigue performance of forged steels.

[36] Borsato, G. et. al. (2020), with the scope of reducing the mass developed a steering knuckle, in Abaqus Tosca, to be produced by additive manufacturing (DLMS). They achieved a model of maraging steel weighing only 4.2 kg, which is only an increase of 0.1 kg from the original aluminum component, having the triple of the density as the initial model. They also mention that it would be possible to achieve a more efficient model,

with the double of the yield limit of the maraging steel if it was submitted to an ageing heat treatment.

[37] Petr, T, et. al. (2020) were able to optimize a knuckle by combining Autodesk Inventor 2020 and Fusion 360. However, the main scope was gaining experience in designing the part, not in the topological optimization itself.

[38] Jasoliva, D. et. al. (2022) combining SolidWorks and HyperWorks were able to optimize a steering knuckle in a way to reduce 60% of the weight, having an increase of 20% on the machining cost when compared to the original design.

[39] Viqaruddin, M. et. Al. (2016), using HyperWorks and Altair, were able to achieve a 41% mass reduction, while decreasing displacement and increasing stifness.

[40] Peng, Y. (2022) performed a mechanical evaluation of a lower control arm, with a 30% mass reduction. It was performed a static and modal analysis before and after optimization to guarantee a better evaluation of the results. The writer also concluded the model was capable of a greater optimization grade.

[41] Harzheim, L. et. Al. (2006) focused on showing original optimization codes for cast parts. The writers introduced software TopShare as it introduces manufacturing constraints.

[42] Darge, S. et. Al. (2014) performed an analysis to the lower control arm of a double wishbone suspension, and optimized the component to reduce stress and, therefore, avoid the cracking and plastic deformation present in the initial geometry.

[43] Bhat, A. et. Al. (2021) implemented Fusion 360 Generative Design as an optimization technique for a lower control arm of a double-wishbone suspension. This technique allowed the removal of 0.46 kg of the total weight, corresponding to a reduction of 51.6%.

[44] Pawar, A. et. al. (2017) used reverse engineering, to create a mesh of an already existing control arm, and, afterwards used software to optimize the model by a reduction in 6.53% of the mass.

3. Planning

The primary objective of this thesis is to create topologically optimized models of two chassis components, aiming to a weight reduction without compromising mechanical properties and safety of the vehicle. To achieve this goal, it is imperative to research the mandatory inputs, such as key points, connections, weight distribution, and loads, among others. Additionally, understanding the appropriate materials selection is crucial since it

directly impacts the cost, geometry, and properties of the model.

The planification of this thesis is set on Figure 4. Conducting a literature survey was essential to withdraw the most used software, materials, loads, and keypoints.

The practical work started by simulating, in Fusion 360, the original geometries, to identify the critical areas and where material redistribution was necessary. Subsequently, various models were generated using "Generative Design" tool. Upon not viable models, simulation conditions were modified until achieving feasible designs.

The iterative approach offers significant advantages by reducing costs, and material waste. Without the use of these tools, companies' profit would decrease, since it would be necessary to produce, wasting time and resources. Through these iterations, it becomes possible to analyze the cost of the final component and make more informed selections regarding the ideal combination of properties and parameters for the intended purpose.

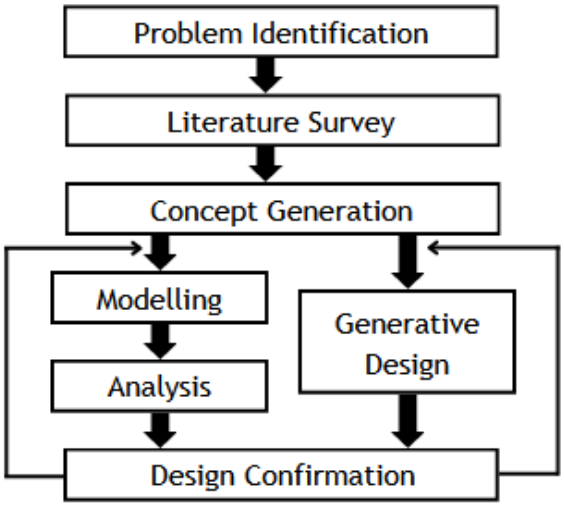


Figure 4 - Methodology

4. Development

There are multiple software used by automotive engineers to test and assess the performance of the components, enabling engineers to identify and correct possible errors in the model. According to Valispace, [45], the primary simulation software in the automotive sector are NX, ANSYS, Solid Edge, and PTC Creo. For prototype design and 3D modelling, Valispace, highlights CATIA, SolidWorks, and Siemens NX.

The chosen software for this thesis was Autodesk Fusion 360, which, although not part of the most used software, allows the user to manage design parameters such as loads, manufacturing constraints, desired performance objectives, and material properties. The software utilizes advanced algorithms to generate optimal design solutions based on the given data. One big advantage of this software is that it generates several results from the same input, allowing the user to choose which design they want given the stress distribution, deformation, or weight, helping engineers understand trade-offs and make informed decisions. Other reasons for the selection of this software were

the possibility to edit and refine the offered results and the reduced time each simulation took considering the number of results it creates [46].

As previously stated, the components will be integrated into a small city car, so they need to be as light as possible, and there is no need to be capable of reaching high velocity. The number of cars to be produced is low, influencing the selection of the manufacturing process and the unitary cost of each component.

As per the specified requirements, CEiiA provided all essential inputs for the study, including load cases, initial models, and keypoints. These critical contributions served as the foundation for conducting a comprehensive and accurate analysis, enabling the study to proceed with the necessary data and information to achieve its objectives.

4.1.Manufacturing methods

Selecting a manufacturing process is a crucial decision influenced by several factors. The chosen process needs to efficiently produce lightweight and durable components while maintaining the necessary structural integrity. The selected process should be cost-effective, allowing the production of a small number of components without compromising quality. The calculation of the cost of each component will be affected not only by the material selection and country of production but also by the manufacturing type.

As mentioned before, the components optimized in this thesis are expected to be produced in a reduced number, so, investing in some manufacturing types may not be cost-effective, for example, in die casting or CPCP, the low number of components may not justify the investment in molds or other necessary materials. Machining, or milling, involves a high amount of material loss, and, with expensive materials, it is a significant waste of cost.

Figure 5 illustrates the relation between unitary cost and part complexity, where it is possible to observe that conventional manufacturing processes, including casting, machining, and milling, have a significant increase in unitary cost with the increase in complexity and a drastic decrease in the number of parts produced. On the other hand, additive manufacturing (AM) processes unitary cost is not influenced by the number of parts produced, and the increase in price due to the complexity is significantly lower than conventional processes [47, 48].

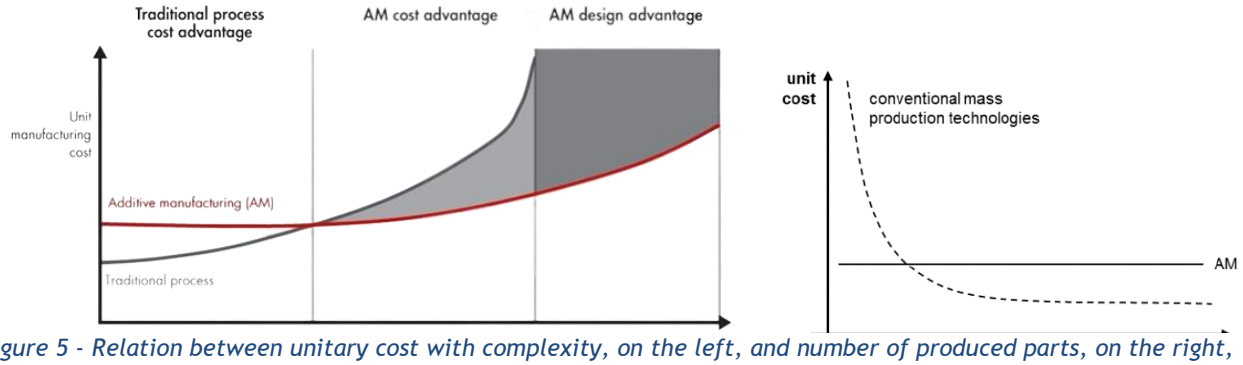


Figure 5 - Relation between unitary cost with complexity, on the left, and number of produced parts, on the right, for conventional and additive manufacturing [47,48]

Fusion 360's Generative design is only capable of simulating the following manufacturing types: unrestricted, for when the manufacturing constraints do not limit the generation of the shape; additive manufacturing, milling, using 2.5, 3 or 5-axis, 2-axis cutting, and, lastly, die casting, however, this is still in development, which can result in not valid results.

4.2.Material Selection

The material selection differs between companies since each tries to develop a new product that is differentiated from the others and according to their market/niche. Deciding on which material to use in the first stages of development has its perks since the design depends entirely on the component's behavior during its lifetime. [SK19]

Not only the material itself and its properties/cost are important, but also the relation with the processing method.

Currently, in the automotive industry, some focus points help guide the material selection, such as reducing emissions, increasing the vehicle's safety, reducing noise and vibration, improving handling, and reducing vehicle costs while increasing the value. As mentioned before, reducing inertia while having great power and less vibration reduces fuel consumption and improves efficiency. These criteria are met by ultra-light materials such as new steels (HSLA, high-strength low-alloy steels), low-cost cast irons (CGI, compacted graphite iron), and aluminum and magnesium components [33].

The research conducted in the literature survey and other sources of information found the most used materials in both components. It was found mainly in three groups of materials, steels, irons, and, more recently, for lightweight purposes, aluminum alloys. Two steels were found, EN8, an unalloyed medium carbon and medium tensile steel, with consistent machining properties and a possibility to enhance wear resistance by surface-hardened induction processes, and EN47, a spring steel applied in the production of spring components, having high strength, good wear resistance, excellent toughness, and good abrasion protection, and high toughness and shock resistance, when they underwent a correct treatment [49 - 60].

Regarding aluminum alloys, it was often used four families, 2XXX, 5XXX, 6XXX, and 7XXX. From the first family mentioned, the addition of 2 to 10% copper increases substantially the strength and enables precipitation hardening, resulting in a reduction of ductility and corrosion resistance, also increasing the risk of solidification cracking. This family includes some of the highest-strength heat-treatable aluminum alloys, however, from the aspects before, some alloys may not be ideal for welding or sealing when exposed to oxidizing elements. From this family, it was distinguished two alloys, 2014 and 2024. The first although suitable for arc welding, is susceptible to corrosion, being applied in frameworks instead of shells, being the second most used alloy in the aerospace industry. The second has high yield strength and is a high-grade alloy with excellent fatigue resistance [61 – 63].

5XXX family has, a major alloying element, magnesium, with moderate to high strength, excellent resistance to corrosion, and readily weldable and non-heat treatable

alloys. It was recognized 5052 alloy since it provides high strength, high ductility, is highly resistant to corrosion, and is used in hydraulic tubes and fuel tanks [64].

From the 6XXX family, it was acknowledged two alloys, 6061, and 6082. The first is very popular for its characteristic toughness in medium- to high-strength applications and for being the most versatile alloy from the family, having increased corrosion to exposed water, snow, salt, sun, and rain due to its additions to this family. 6082 is a structural alloy, providing one of the highest strengths of the family, being a good alternative for 2XXX or 7XXX series, since they can be extruded into more shapes than them. It is known for its machining, weldability, cold formability, and corrosion resistance. The addition of manganese helps to control the grain structure, allowing it to be applied in applications where it is required strength and toughness. However, it is harder to extrude thin-walled complex geometries than in other alloys within this family. This being said, the addition of silicon and magnesium combined with heat treating or cold working allows this family to be easily anodized, and, for some grades, excellent spot and fusing weldability [65 – 67].

Lastly, the 7XXX family is the series with the highest strength of all series, having zinc as the primary alloying element. It has excellent fatigue properties but is only able to be spot welded, never fusion welded. To be protected of corrosion it needs to be anodized, primed, painted, or protected by chemical films. It was detected three major alloys 7050, 7068, and 7075. The first has a combination of high strength, fatigue, and resistance to stress corrosion cracking. The second is one of the strongest alloys of aluminum, able to match certain steels, and also has a yield strength up to 700 MPa (30% over 7075) and good ductility. As for 7075, similarly to 7068, its strength can also be compared to steel, it has impeccable fatigue resistance, is easy to machine, has incredible stress corrosion resistance, and provides high yield and tensile strengths. It is mostly when corrosion resistance is non-essential, and it is needed [68 – 72].

To compare all the above-mentioned materials, it was utilized the software Granta EduPack 2022 R2 Level 3. The most important factors for these components' applications are the price since it will influence the cost of the piece and mechanical properties. In this software's database, it was also pursued an analysis to learn if the chosen materials are suitable for casting, weldability, and sheet metal [73].

Figure 6 is a comparison of the price of all materials with mechanical properties such as Yield strength, Young modulus, and density. Table 1 has all this data, however, in more detail. By Granta's definition "Excellent is for when the material is frequently used for the method and does not present any major problems, acceptable for when the material is generally used, but may not be an optimized grade, limited use when the material may be used in limited cases, or requires additional measures to avoid problems, and unsuitable for when the material is not used for the method in study" [73].

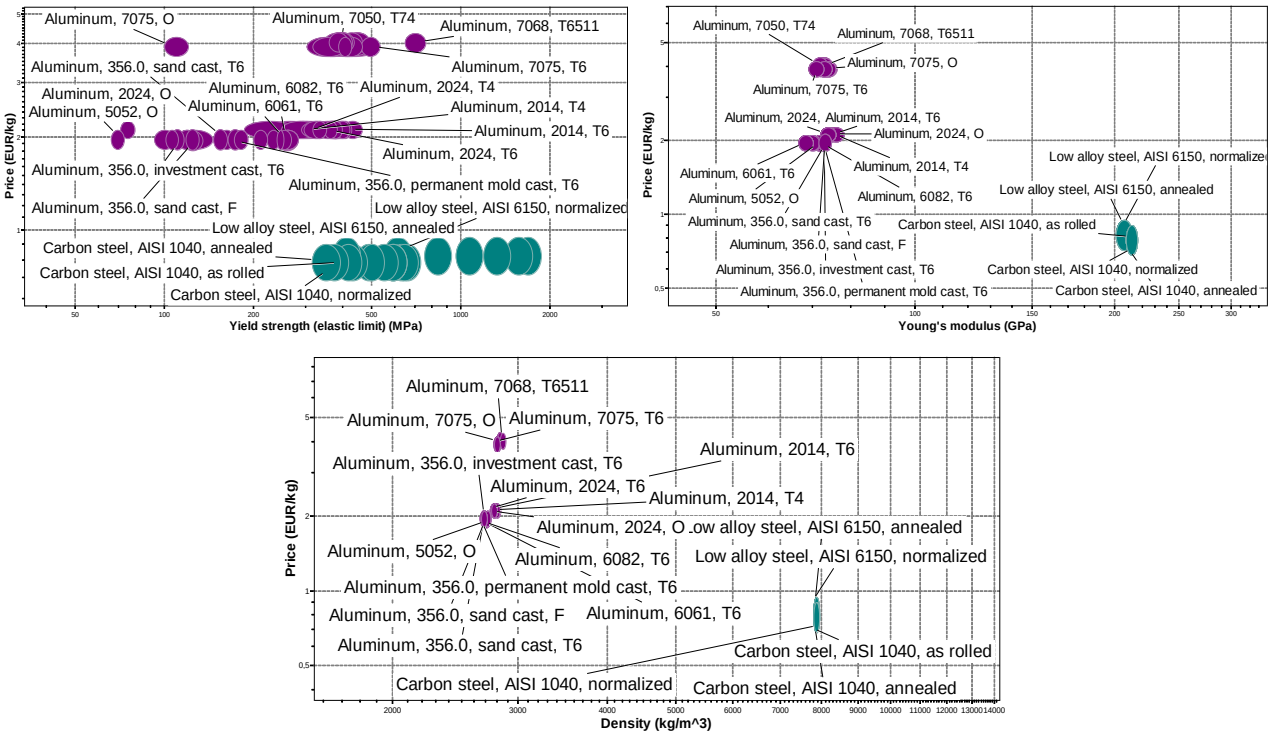


Figure 6 - Materials Properties, Retrieved form [73]

Table 1 - Materials Properties, Retrieved from [73]

Material		Casting	Weldability	Price (€/kg)	Density	Young's Modulus (Gpa)	Yield Strength (Mpa)
EN8 AISI 1040	Normalized	Unsuitable	Good	0.687 - 0.091	7.8e3 - 7.9e3	208 - 216	335 - 415
	Annealed						315 - 390
EN47 AISI 6150	Normalized	Unsuitable	Good	0.719 - 0.946	7.8e3 - 7.9e3	201 - 212	550 - 680
	Annealed						370 - 455
2014 T6		Unsuitable	Excellent	1.98 - 2.25	2.77e3 - 2.83e3	72 - 77	324 - 440
2024 T6		Unsuitable	Unsuitable	1.98 - 2.25	2.75e3 - 2.78e3	72 - 75.7	345 - 381
5052, O		Unsuitable	Good	1.83 - 2.1	2.67e3 - 2.7e3	70 -73.6	66 - 72.9
6061 T6		Unsuitable	Good	1.83 - 2.1	2.67e3 - 2.7e4	66.6 - 70	240 - 280
6082 T6		Unsuitable	Good	1.81 - 2.09	2.67e3 - 2.7e5	70 - 74	240 - 280
7050 T74		Unsuitable	Poor	3.77 - 4.35	2.81e3 - 2.84e3	70 - 73.6	372 - 427
7068 T6511		Unsuitable	Unsuitable	3.76 - 4.33	2.85e3	70 - 73.6	648 - 756
7075		Unsuitable	Unsuitable	3.66 - 4.2	2.77e3 - 2.83e3	69 - 76	460 - 530
A356.6		Excellent	Excellent	1.82 - 2.12	2.66e3 - 2.71e3	71.5 - 74.5	118 - 130
AlSi10Mg (A360.0)		Excellent	Excellent	1.82 - 2.13	2.66e3 - 2.71e4	69.6 - 72.4	157 - 173

4.3. Geometry Requirements

A vehicle's front wheels are mounted in a way so that they can pivot about a vertical steering axis, having an additional degree of freedom. A good steering system is also responsible for transmitting feedback from the roads to the driver, allowing an appropriate response to the road condition among the usual change of direction [1].

The main components of each assembly are present in Figure 7 (some elements are hidden to allow a better understanding of each geometry):

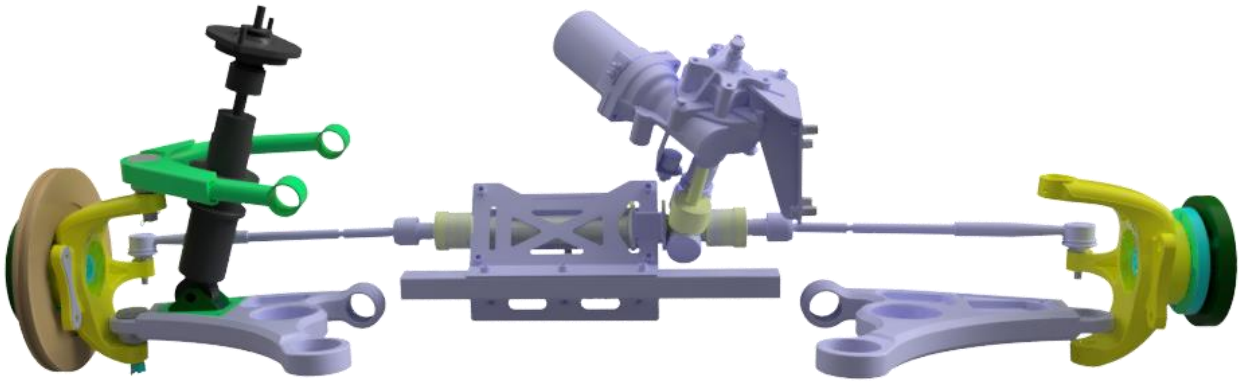


Figure 7 - Steering system assembly

In more detail in Figure 8, the components corresponding to the front right wheel, the components in study are as follow:

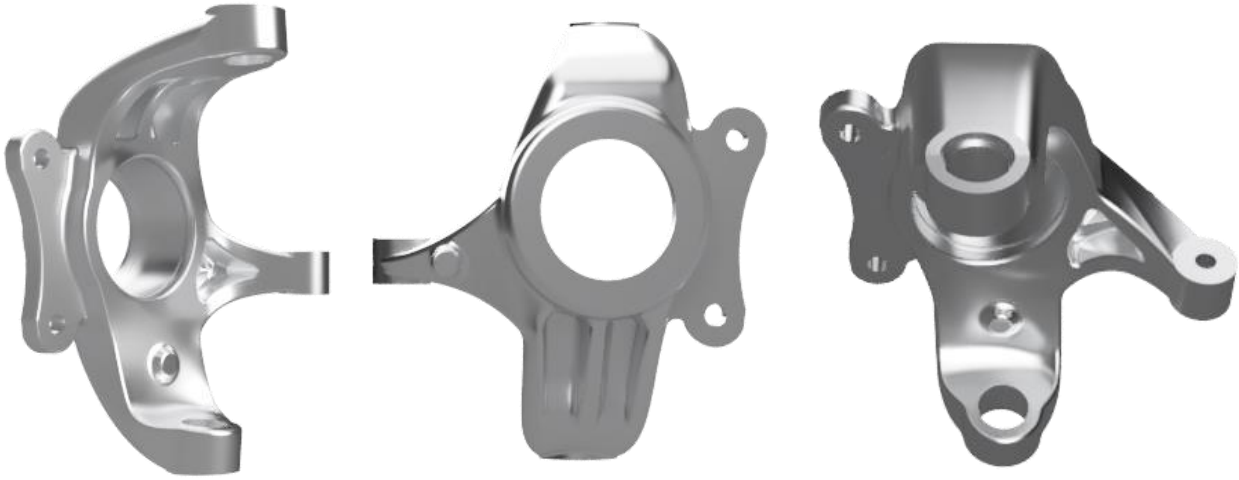


Figure 8 - Steering system detailed

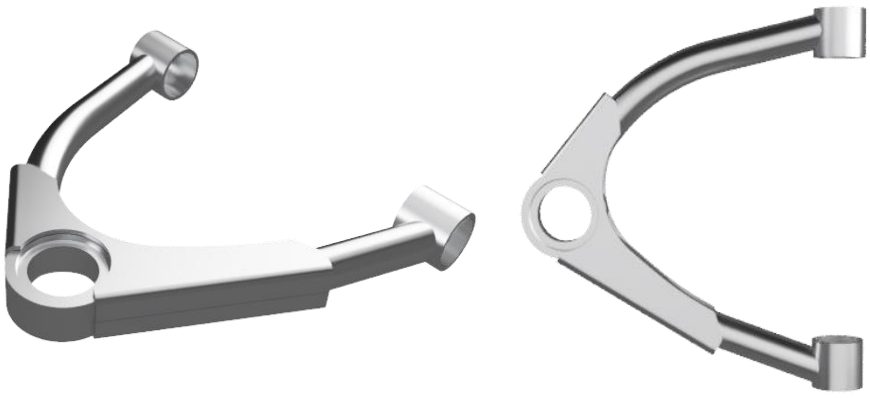
The components in study are, in yellow, the steering knuckle, and, in lighter green, the upper control arm, Figure 8.

These geometries already consider requirements such as driving dynamics, ride comfort, chassis weight, cost, reliability, and durability, vehicle performance, steering while braking forces, among others.

Figure 9 and Attachment 1, show, in more detail, the original geometries of the components in study, provided by CEiiA.



(a) Steering Knuckle

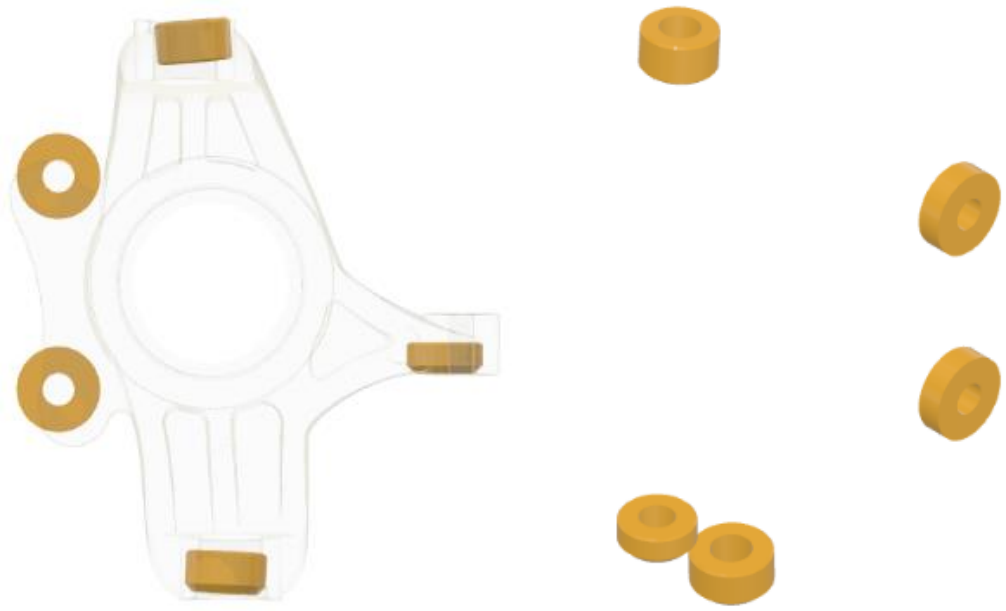


(b) Control arm

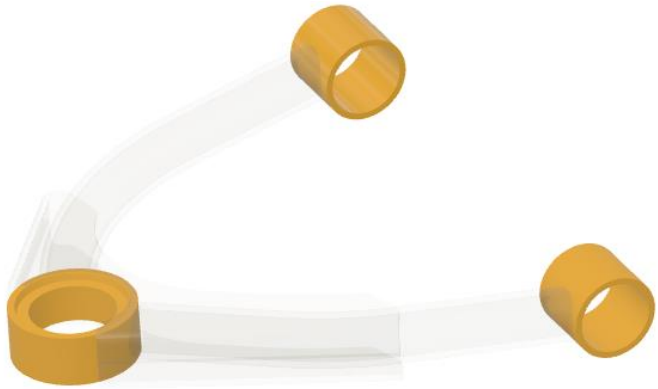
Figure 9 - Component's initial geometry

Any geometry can be divided into two segments, the design space, and the non-design space. The non-design geometries of the steering knuckle and control arm are shown in Figures 10 a) and b) respectively. These correspond to the key points, where the loads are applied, and geometries that cannot be changed. The design space is defined as

the closed volume that will be subjected to topology optimization, being the one to be redesigned according to the desired goals [14, 17].



(a) Steering Knuckle



(b) Control arm

Figure 10 - Non-Design space of each component

4.4. Definition of Loads

The load cases were provided by CEiiA, where all the restrictions and conditions were taken into consideration. The literature survey was also used to verify the given load cases. There will be tested four conditions, front wheel over bump, lateral curb strike, reverse bump, and panic braking.

Front wheel overbump corresponds to an analysis when the vehicle is driving over any type of bumps. These are important analysis since, when the wheel crosses the bump, it starts to ascend towards the chassis, compressing the suspension.

Lateral curb strike relates to a significant impact on the lateral of the car.

Reverse Bump simulates the movement of a wheel driving through a bump while in reverse.

Panic braking correspond to an "emergency stop" where there is a large load transfer in the movement direction.

For the control arms study it will only be utilized one set of load cases, however, for the steering knuckle, there are two sets of load cases, being one more complete than the other.

Table 2 - Load Cases 1 applied to the Steering Knuckle

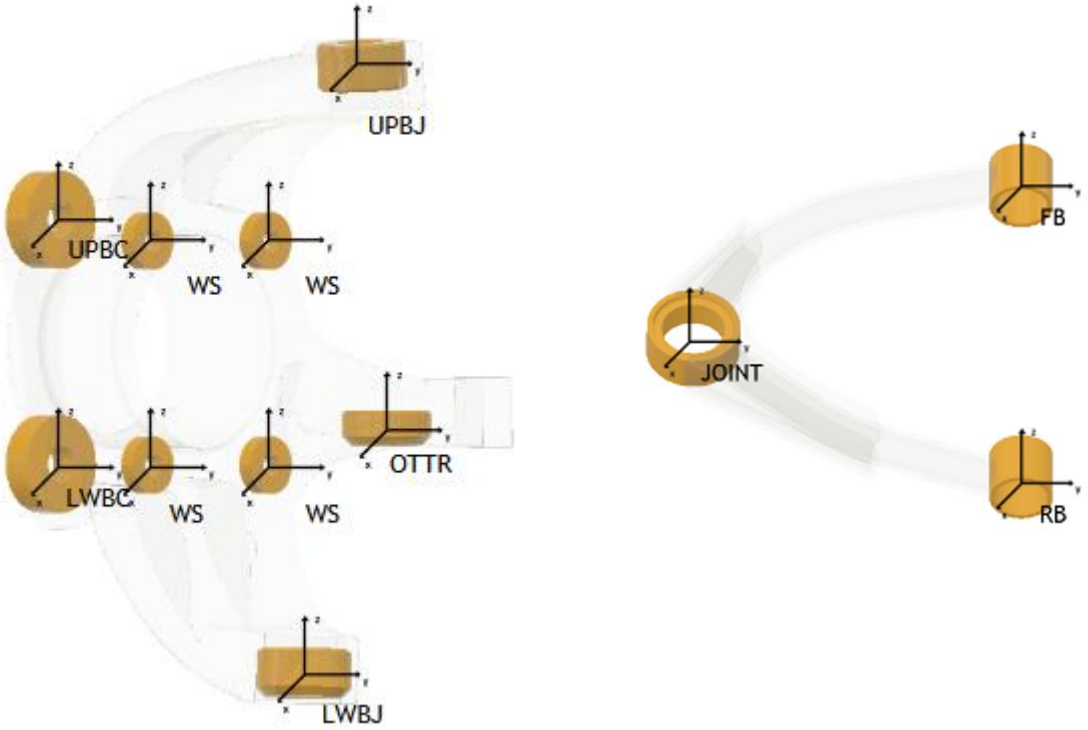
Steering Knuckle		FWOB			CURB			RB		
		Fx (N)	Fy (N)	Fz (N)	Fx (N)	Fy (N)	FZ (N)	Fx (N)	Fy (N)	Fz (N)
1	**UPBJ**	5290	-2580	332	25,6	5720	-1930	699	-813	125
	LWBJ	-9860	2230	-7440	232	-14800	-1310	1340	1240	-3200
	OTTR	-56.8	349	-63.9	-257	1690	-1930	64.6	-428	48.6
	UPBC	2000*								
	LWBC									
*only from simulation number 7 onwards.										
UPBJ - Upper ball joint | LWBJ - Lower ball joint | OTTR - Outer tied rod | WS - Wheel Spindle										

Table 3 - Load Cases 2 applied to the Steering Knuckle

Steering Knuckle		FWOB			CURB			PB		
		Fx (N)	Fy (N)	Fz (N)	Fx (N)	Fy (N)	FZ (N)	Fx (N)	Fy (N)	Fz (N)
2	**UPBJ**	-7489.89	3817.56	-927.075	-42.2953	-6818.96	2853.59	-7379.87	3329.84	-568.176
	LWBJ	13783.4	-3422.39	11744.3	-280.359	18354.6	2909.21	13643.8	-2758.3	9768.93
	OTTR	70,1776	-395.171	92.0491	322.655	-1990.02	373.643	99.7621	-571.539	118,1
	WS	-6363.73	0	-11031.6	0	-9545.59	-6258.75	-6363.73	0	-9440.62
	UPBC	2000								
	LWBC									
UPBJ - Upper ball joint | LWBJ - Lower ball joint | OTTR - Outer tied rod | WS - Wheel Spindle										

Table 4 - Load Cases applied to the Control arm

Control Arm	FWOB			CURB			PB		
	Fx (N)	Fy (N)	Fz (N)	Fx (N)	Fy (N)	FZ (N)	Fx (N)	Fy (N)	Fz (N)
Front bush	-3978.08	7470.15	-3186.69	-38.572	-2909.34	1219.87	-3902.25	7284.62	-2768.81
Rear Bush	-3511.8	-3652.59	2244.89	-3.72332	-3909.62	1619	-3477.61	-3954.78	2185.37
Joint	7489.89	-3817.56	42927.075	42.2953	6818.96	-2853.59	7379.87	-3329.84	568.716



(a) Steering Knuckle *(b) Control arm*

Figure 11 - Load Points

Among these loads, it is also mandatory to have a factor of safety of 2. The factor of safety (FoS) is an indicator of the structural capacity of the component to behave in the application of loads. It is expressed as a ratio that compares absolute strength to the actual applied load. Ideally, it is calculated by the division between the maximum stress and the working or design stress. However, in substitution of maximum stress, for brittle materials, ultimate stress determines the FoS until failure, and, for ductile materials, yield stress determines the FoS until the beginning of deformation. Higher numbers are expected for a safer product or structure. For values of 1 or lower, the component will fail immediately, and it is not able to support any extra load, enabling it. Therefore, values of FoS below 1 are not acceptable. Depending on the application of a component, there are stipulated minimum values of FoS, for example, if used in components that, in case of failure, will result in injuries or loss of life, it is required, by law, a higher value of FoS. Also, regarding the cost, with the increase of the FoS, the cost of the product is also increased, mainly because it requires an extra amount of material. When designed, for safety, any component must endure higher loads or corrosion resistance than it would need in normal settings [74 – 77].

5. Simulations

CEiiA provided the initial models and load requirements for the study. The obstacles used in the analysis were carefully designed, considering the provided models and applying a tolerance to ensure a simplified approach and minimize the risk of solver errors. Furthermore, the loads were accurately applied at the center of ball joints to ensure precise and reliable results.

5.1. Fusion 360 Generative Design

Generative Design concept has set a new worldview during the prototyping periods of automotive parts. When a component is being designed in the manufacturing industry, the designers input the required objectives into the design program. For higher quality results, there are other inputs as boundary constraints, such as manufacturing processes, and design space, among others shown in Figure 12.

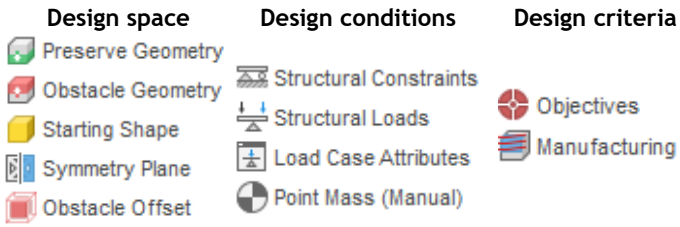


Figure 12 - Generative Design available inputs

This function is very diverse, allowing the user to set several restrictions, such as preserving geometries, representing the non-design area, and the obstacles, corresponding to the other components present in the suspension. As for the starting shape, this is a non-mandatory input, but it can serve as a guideline for the solver to create new models. Regarding the load inputs, there are structural constraints applied to the preserved bodies and fixed in the design. The structural loads are the most important aspect since they are the focus of the solver when creating the new geometry. Lastly, it is necessary to select the materials used in the study and the objectives. The objectives correspond to the definition of the factor of safety is defined, the main goal can be either to minimize the mass or maximize stiffness, and the maximum displacement allowed. It is also possible to select the manufacturing type if it is unrestricted, milling, 2-axis cutting, or die casting. However, die casting, as of June 2023, is still under development, allowing for possible errors in the creation of results [43, 46].

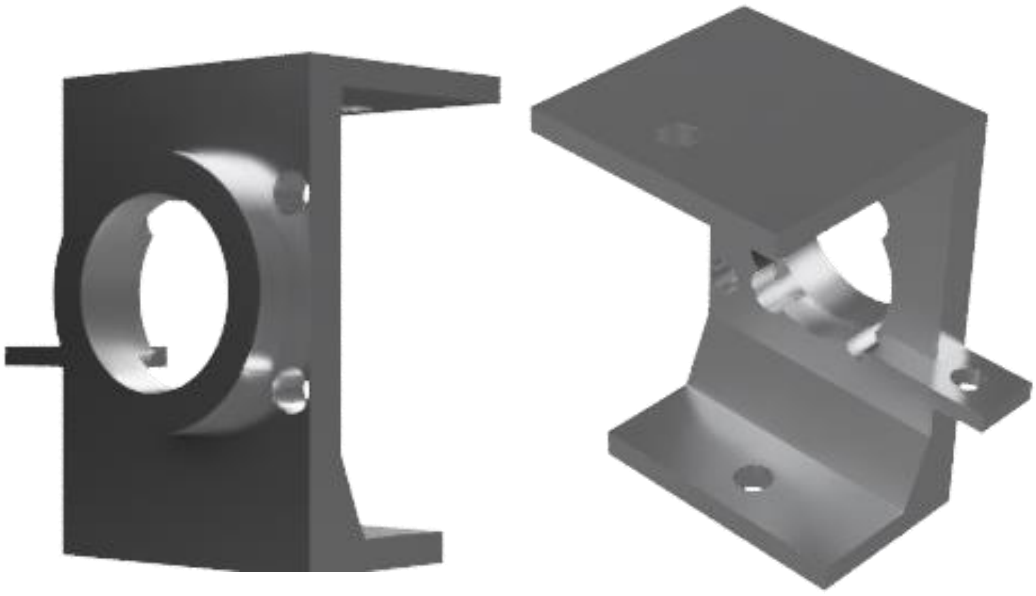
In contrast with other topological optimization software, Fusion's Generative Design explores multiple solutions, providing design alternatives in a reduced time of simulation.

5.2. Steering Knuckle

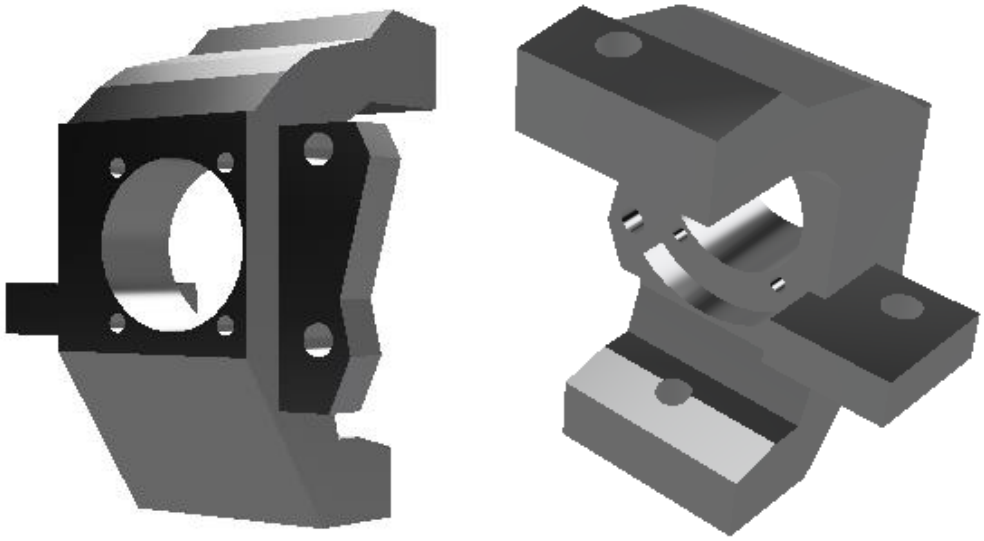
5.2.1. First Geometry

To begin the simulations for both components, it was essential to analyze the given model and its constraints, to determine the areas where optimization was needed.

As for the steering knuckle, the provided model had misplaced keypoints, prompting the creation of two alternative models with similar dimensions but correctly positioned keypoints, Figure 13, to simulate the new positions. These models were then used to simulate the loads in the original design for comparison and further analysis.



(a) "Simple" Geometry



(b) "Bulk" Geometry

Figure 13 - Component's alternative initial geometry

The results were conducted in two materials, A356 T6, since ir was the original material, and due to its low young modulus and yield strength, and 2014, since it has a similar young modulus but higher yield strength. It was not possible to simulate any of the steels since they were not present in Fusion 360 database. The results are displayed in Table 5.

Table 5 - First analysis results

		Factor of Safety			Stress (MPa)		Displacement (mm)	
		min		max	min	max	min	max
		A356 T6	2014 T6					
Given	FWOB	1.153	2.794	15	0.01994	143.1	0	0.423
	CURB	0.4616	1.119	15	0.1023	357.4	0	0.7468
	RB	3.589	8.697	15	0.00419	45.98	0	0.1311
created "simple"	FWOB	2.879	6.977	15	0.006391	57.32	0	0.1409
	CURB	4.212	10.21	15	0.01263	39.17	0	0.4138
	RB	6.874	15	15	0.003456	24	0	0.06
created "bulk"	FWOB	0.9752	2.363	15	0.03174	169.2	0	0.09981
	CURB	0.7518	1.822	15	0.0639	219.5	0	0.1827
	RB	4.493	10.89	15	0.0101	36.72	0	0.0324
FWOB - Front wheel overbump | CURB - Lateral Curve Strike | RB - Reverse Bump								

The results of each simulation follow a color gradient to indicate the Factor of Safety. The software considers values of FoS above 3 as safe, being represented by green if they are lower than 6 and blue if they are above. Between 1 and 3, the component is represented by yellow, indicating it may not withstand the applied loads, and red for values below 1, when it is assumed that the component will break or crack.

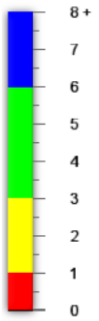


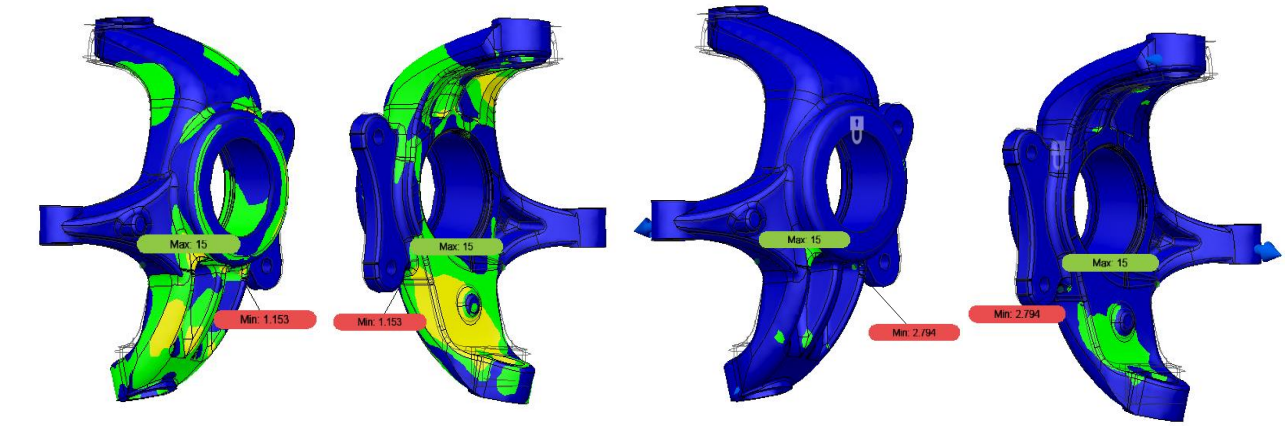
Figure 14 - Results Color Gradient

From both A356 and 2014 results, only the simpler model successfully had a factor of safety over 2 in all three simulations; however, the value of FoS is always higher in 2014 T6. The rest of the results were not affected by the selection of the material. As the deformation is reduced, all the figures were taken with an adjustment of 5% of the deformation to understand where the component moves.

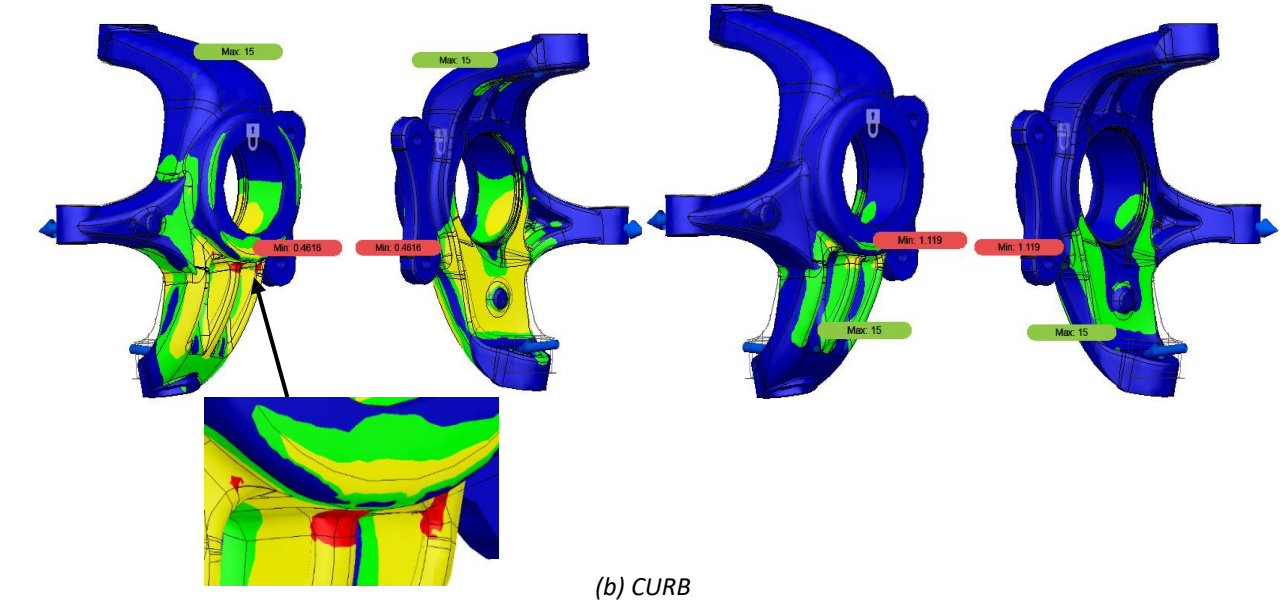
The results of the given model are displayed in Figures 15, 16. As it is possible to observe, almost all the component is graded in blue, with the highest amount of stress focused on the "cuttings" of the model, as detailed in Figure 15b. It is more pronounced in the lateral curve strike analysis, displaying a FoS lower than 1 in A356.

The displacement is higher in the first case, the front wheel overbump study, being detected both in the upper and lower body, although, as in the other models, it is significantly higher in the lower section.

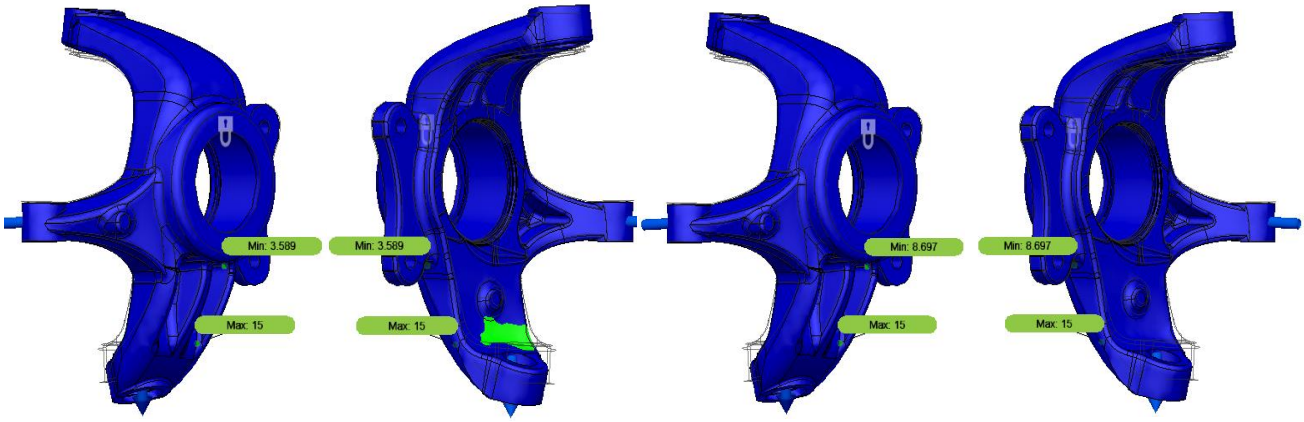
Overall, all three simulations show major stress in the lower region of the component.



(a) FWOB

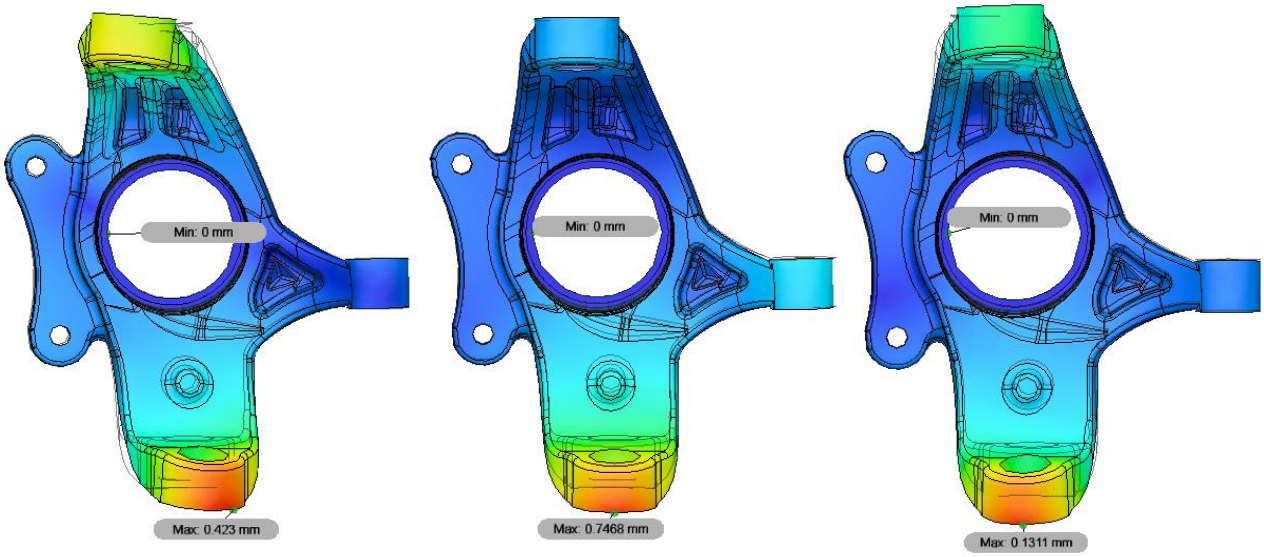


(b) CURB

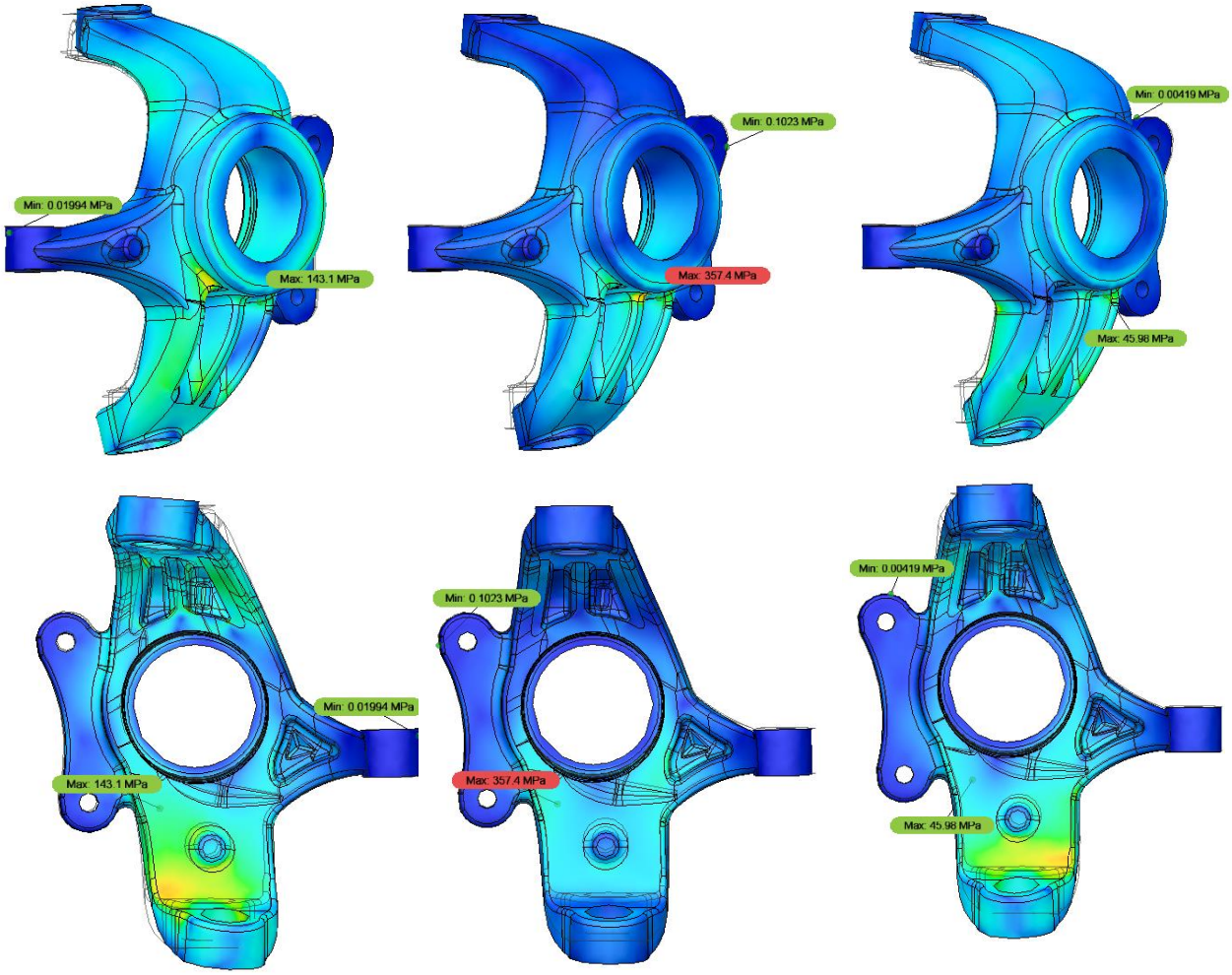


(c) RB

Figure 15 - Initial geometry - FoS simulation results



(a) Displacement

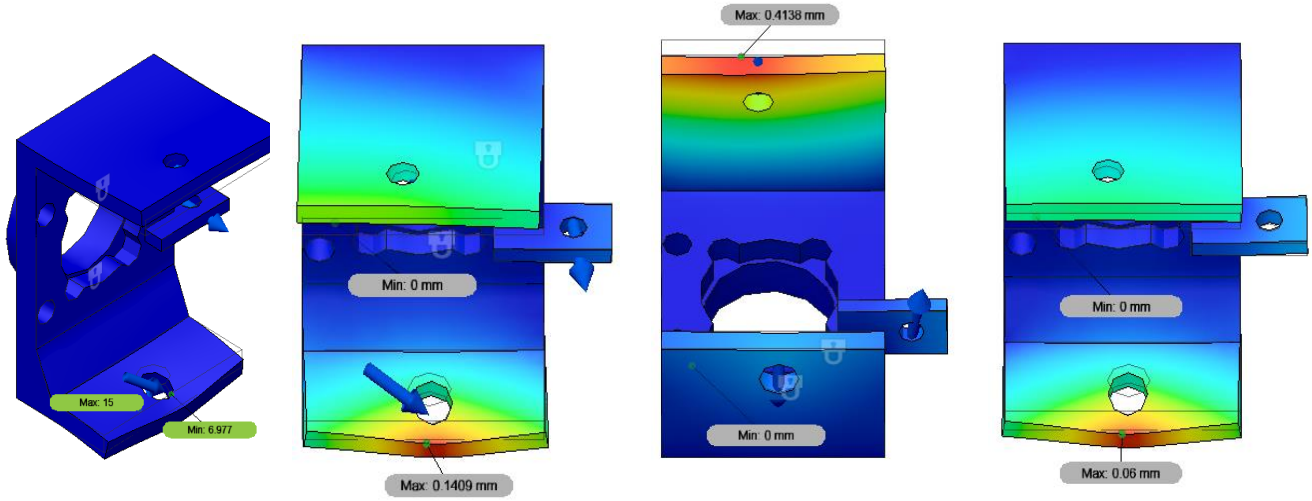


(b) Stress

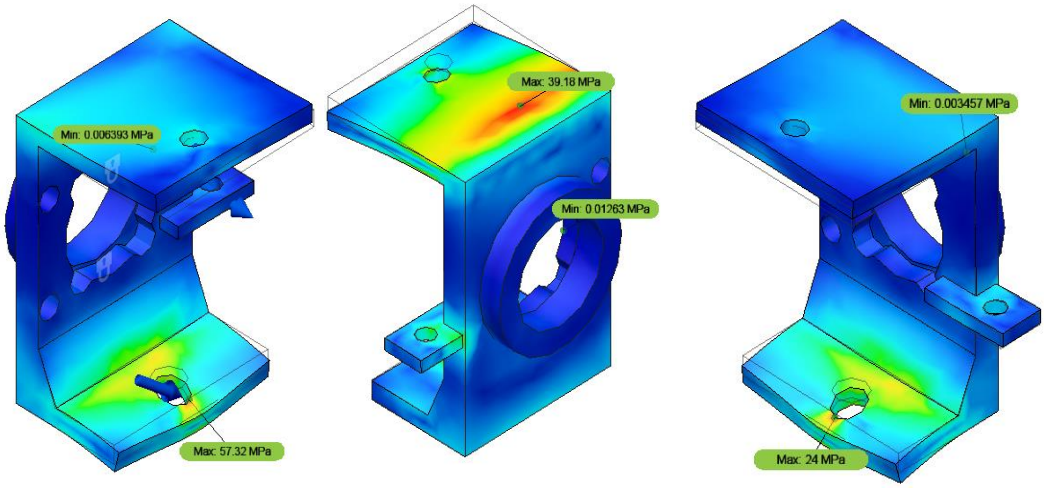
Figure 16 - Initial geometry - Displacement and Stress simulation results

Both the simpler and bulkier-shaped models were designed taking into consideration the original designs. Although the keypoints are at the correct points and do not intersect obstacle bodies, it is important to mention that the remaining dimensions, such as length and thickness, were eyeballed, so the results just take into consideration the load on different types of models, making a critical analysis of the results necessary.

For the simpler shape, as shown in Figure 17, the critical points are located near the lower and upper keypoints. Both the reverse bump and wheel overbump simulations have nearly all the tension and displacement in the lower section of the body, while the lateral curve strike has a higher displacement than the other two simulations, and it is possible to observe stress in the body, not only in the keypoint cuts as in the other two.



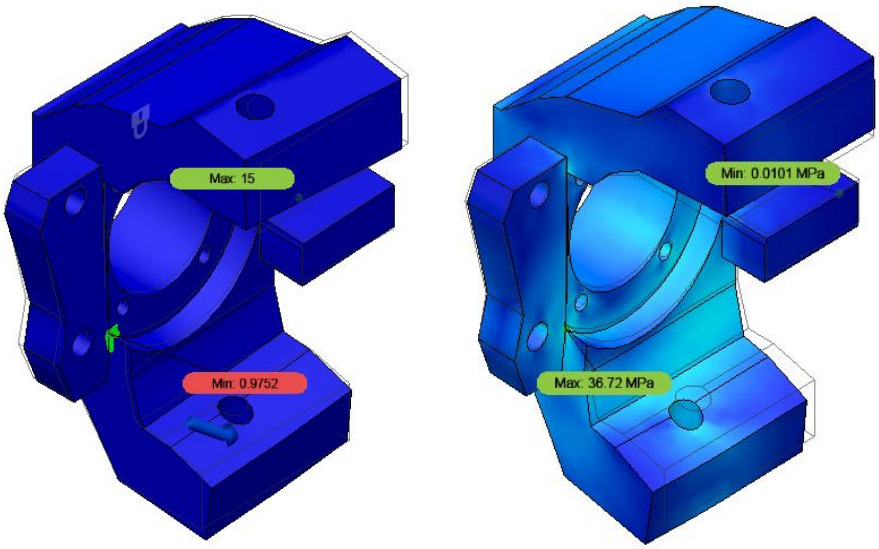
(a) Displacement



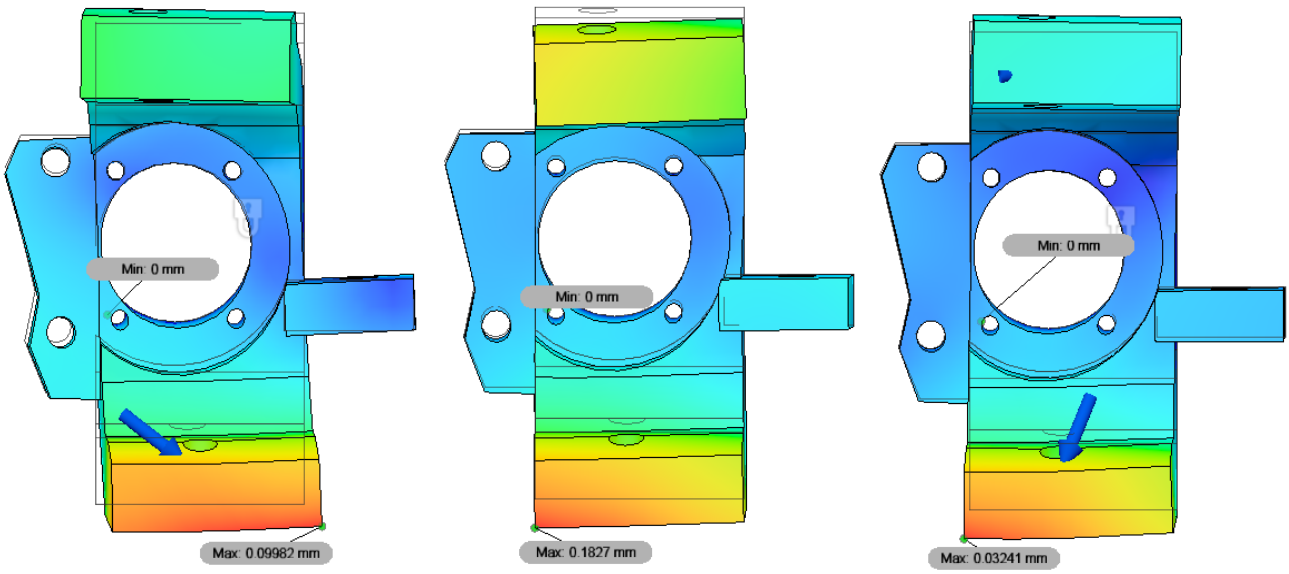
(b) Stress

Figure 17 - Simpler geometry - Displacement and Stress simulation results

Regarding the box-shaped results, since the dimensions were created without a lot of detail, the stresses were focused on a specific point corresponding to an, however, the rest of the model did not detect any significant tension or displacement. As one of the goals is to achieve a lightweight model and reduce the mass of the initial model, this is not an ideal shape. However, if this was not a requirement, after optimization, this could be a usable shape.



(a) Stress



(b) Displacement

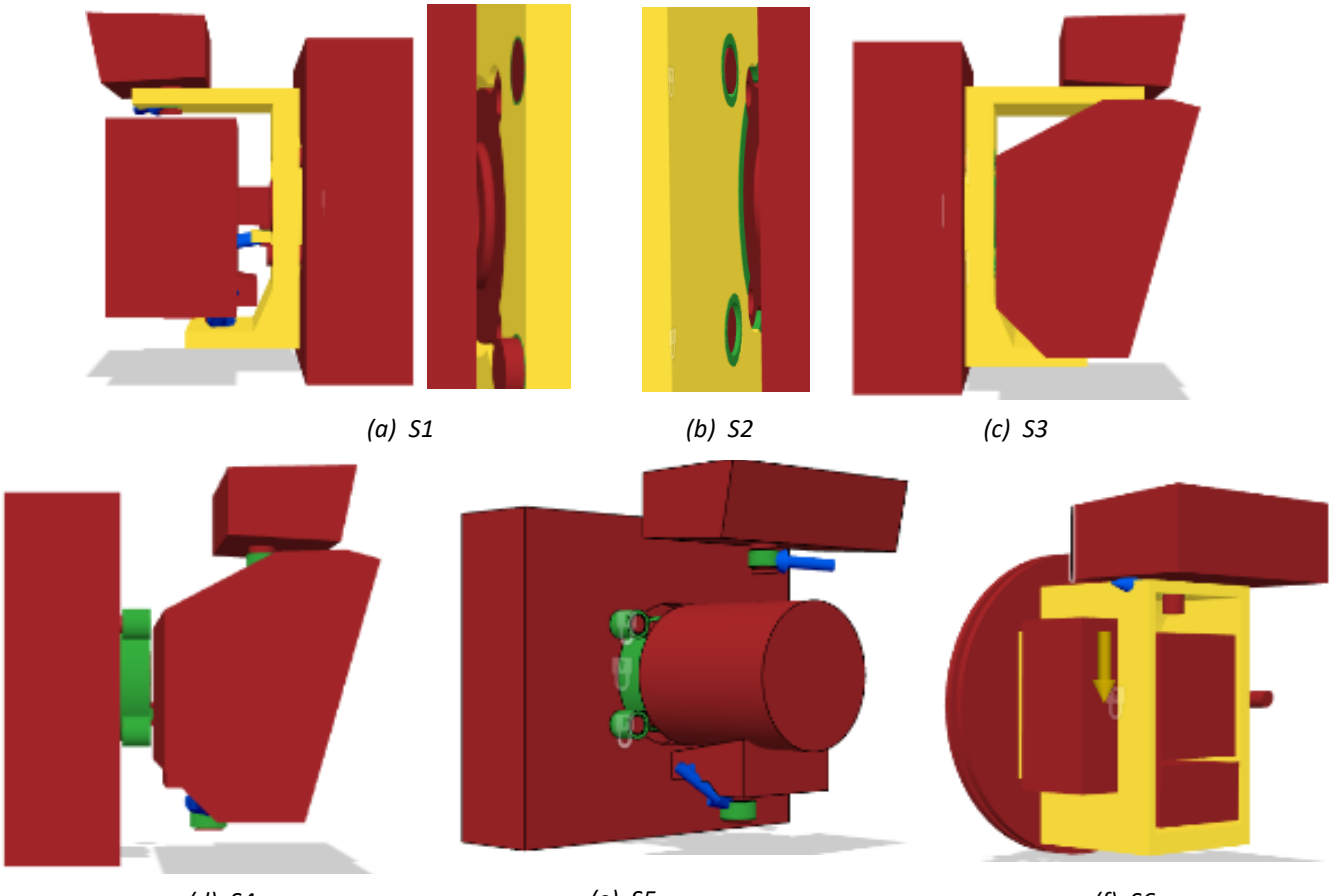
Figure 18 - "Bulk" geometry - Displacement and Stress simulation results

5.2.2. Designs created by Generative Design

The simulation-based optimization techniques employed a trial-and-error methodology. As this is a crucial and complex component, the deepening of its understanding leads to a trial-and-error methodology, leading to the creation of invalid simulations. Even though these simulations did not provide valid results for topologically optimized outcomes, they will be detailed in this thesis as a method to validate the utilized software. Each simulation is identified by S and its respective number, and, Table 6, is the summary of all the simulations decisions.

S1 and S2 were the first simulations to be produced for Generative Design. The obstacles and initial body are the same, differing only in the size of the preserved bodies, which have larger dimensions in S2. S3 kept the preserved bodies and first geometry from the previous simulation, increasing the obstacles bodies, as demonstrated in the Figure.

S1, S2, and S3 had the same initial body as a method to indicate to the solver the path where the steering knuckle should be created. S4 kept the same bodies as S3, except for the initial body, to evaluate if the solver would present any different solutions. The alteration from S4 to S5 was only in the central obstacle, adopting a cylindric shape to minimize rough edges in the outcomes. S6 was created based on the geometry found on an article, which was rejected for not taking into consideration the movement of the lower control arm.



(a) S1 *(b) S2* *(c) S3*

(d) S4 *(e) S5* *(f) S6*

Figure 19 - Simulations S1 - S6

Up to this point, all the generated results lack a connection between the keypoints of the caliper and the main body, as it is possible to observe in the following example. Although the solver detects the results as valid, there were simulated new designs with the hope of achieving results with a connection.

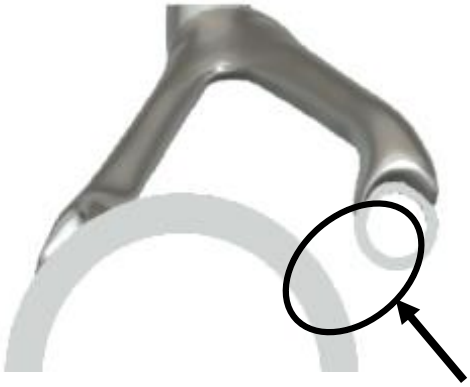


Figure 20 - Lack of connection present in the generated results

With the aim of achieving a connection, from S7 onwards, a load of over 2000 N was applied to both keypoints of the caliper. Compared to S5, S7 does not have any geometric difference. As it is possible to observe in the Figure, the application of loads did not achieve the goal, so it was created two models, S8 and S9, with already a connection between the keypoints and the main body, differing on the diameter of the connection. As it is possible to observe in Figure 21, S9 has the better design results since S8 did not complete the integration of the created connection. However, the lower section is still not ideal.

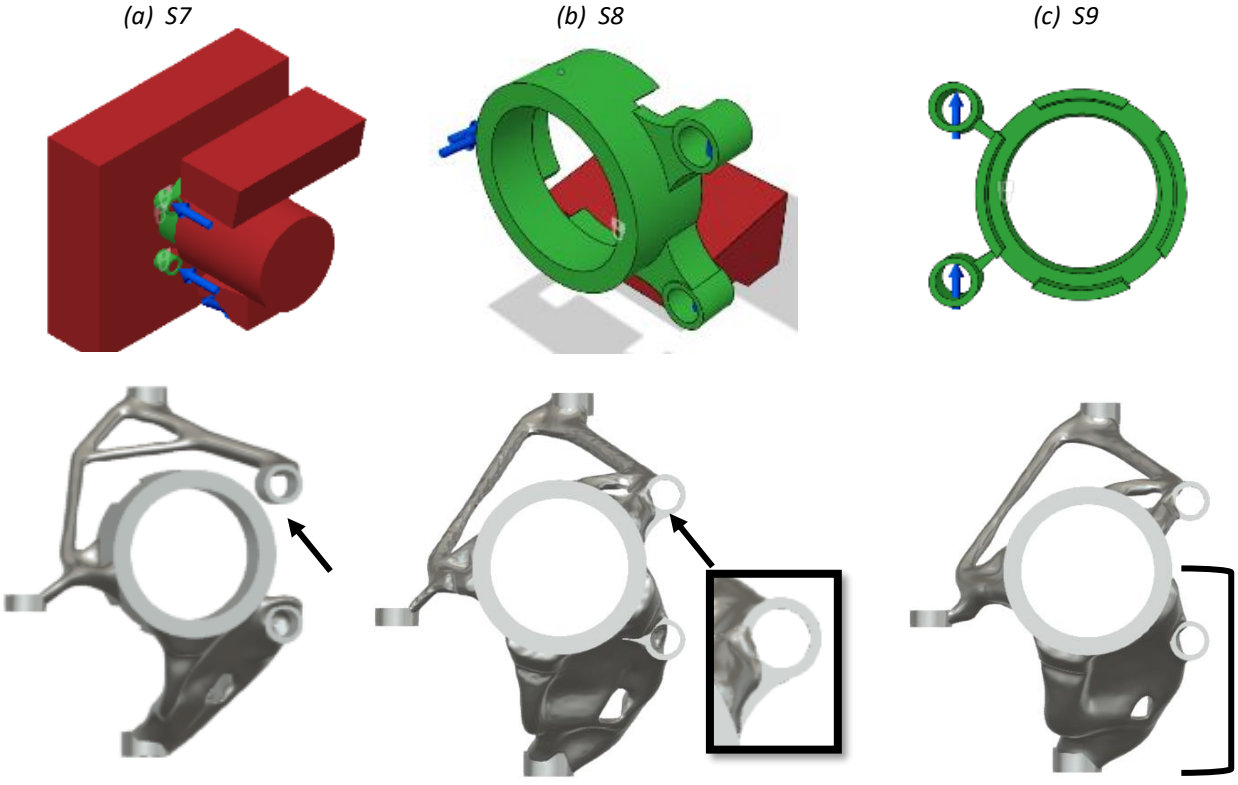


Figure 21 - Simulations S7 - S9

At this point it was detected an incorrect read of the assembly of the component, so, only from this point, the results can be considerate for the final topological optimized model.

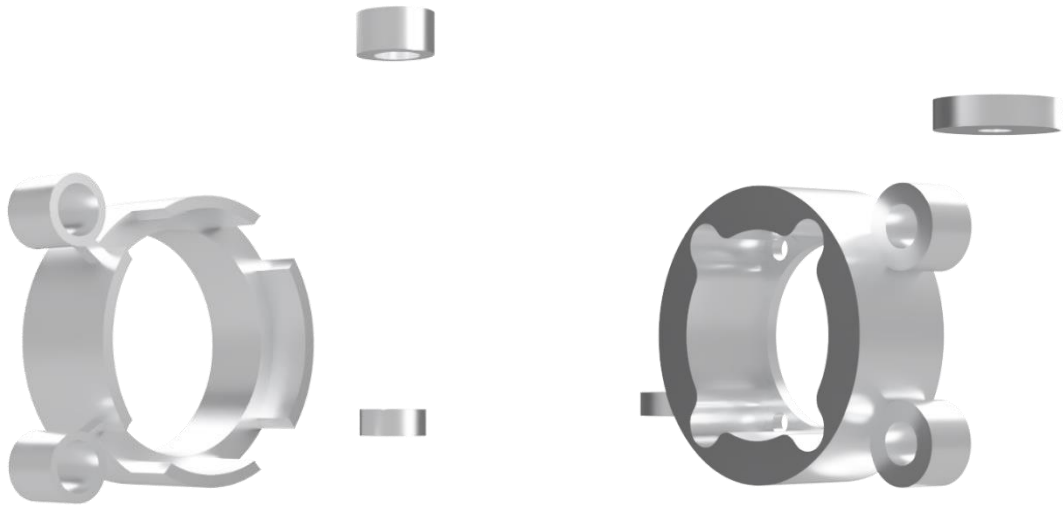


Figure 22 - Geometry Correction

Alongside this correction, it was also created a new obstacle, taking into consideration the movement of the lower control arm.



Figure 23 - Lower Control arm movement

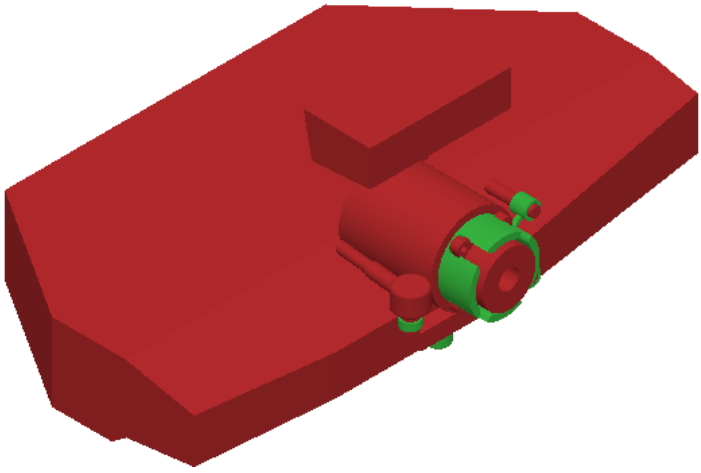


Figure 24 - S10

Regarding S10 results, upon selecting all the keypoints as constraints, any of the produced results were valid. All the outcomes with the status "completed" had a warning about the separation of the bodies, as shown in Figure 25. When reducing the constraints to only the front face of the central body, several interesting results appear.

It is also relevant to mention that all the results displayed are as given by the solver; they were not submitted to the available optimization steps such as smooth and cylindrify, among others, justifying the rough visual appearance.

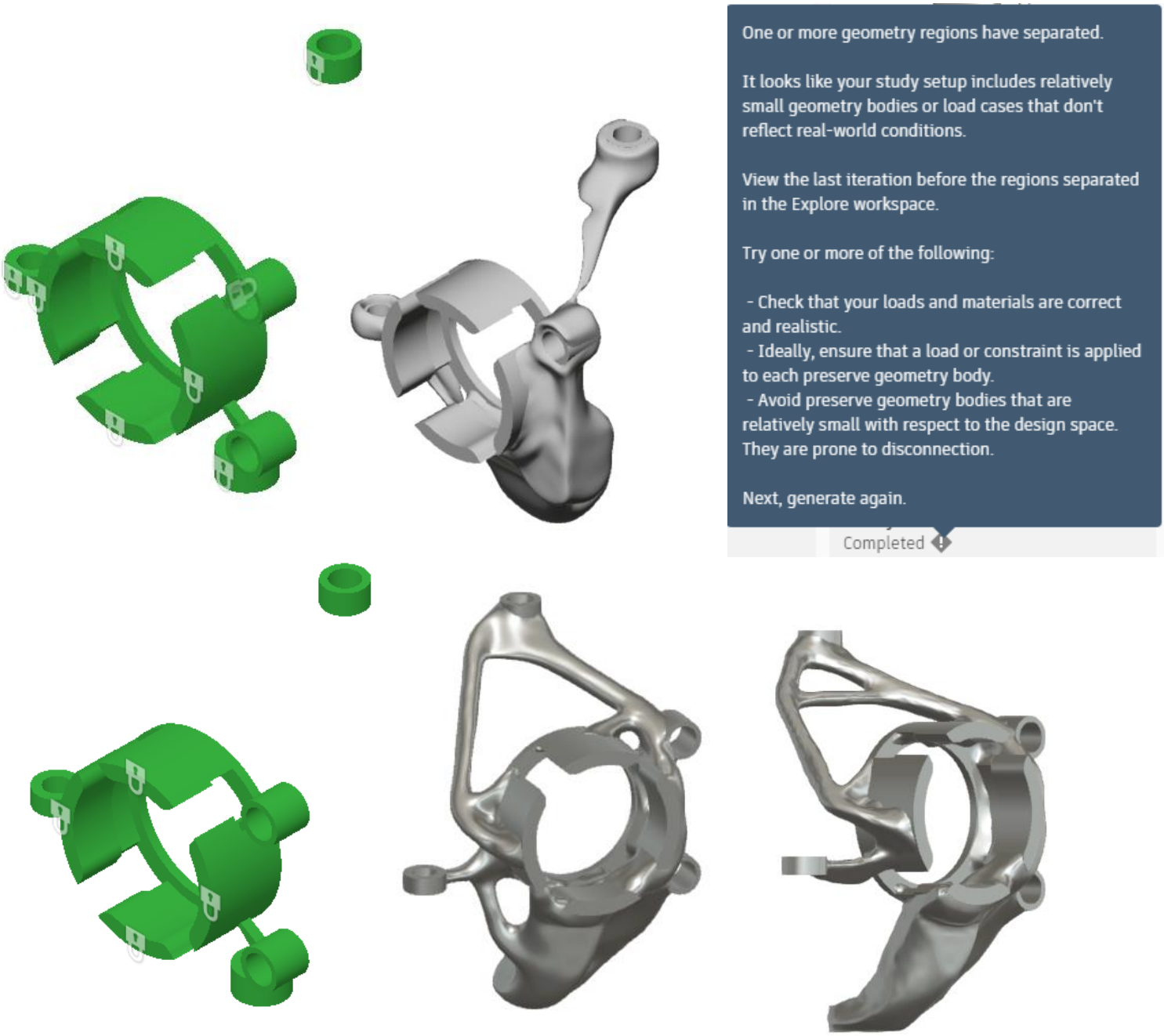


Figure 25 - S10 results

To understand if the "wall" thickness in S10 influenced the results, the thickness of the central body in S11 was increased. Regarding these results, the same error as in S10 occurs; there is a message of error when attributing constraints to all keypoints; however, when only the front face of the central body is selected, the solver generates several great outcomes on the top region, design-wise.

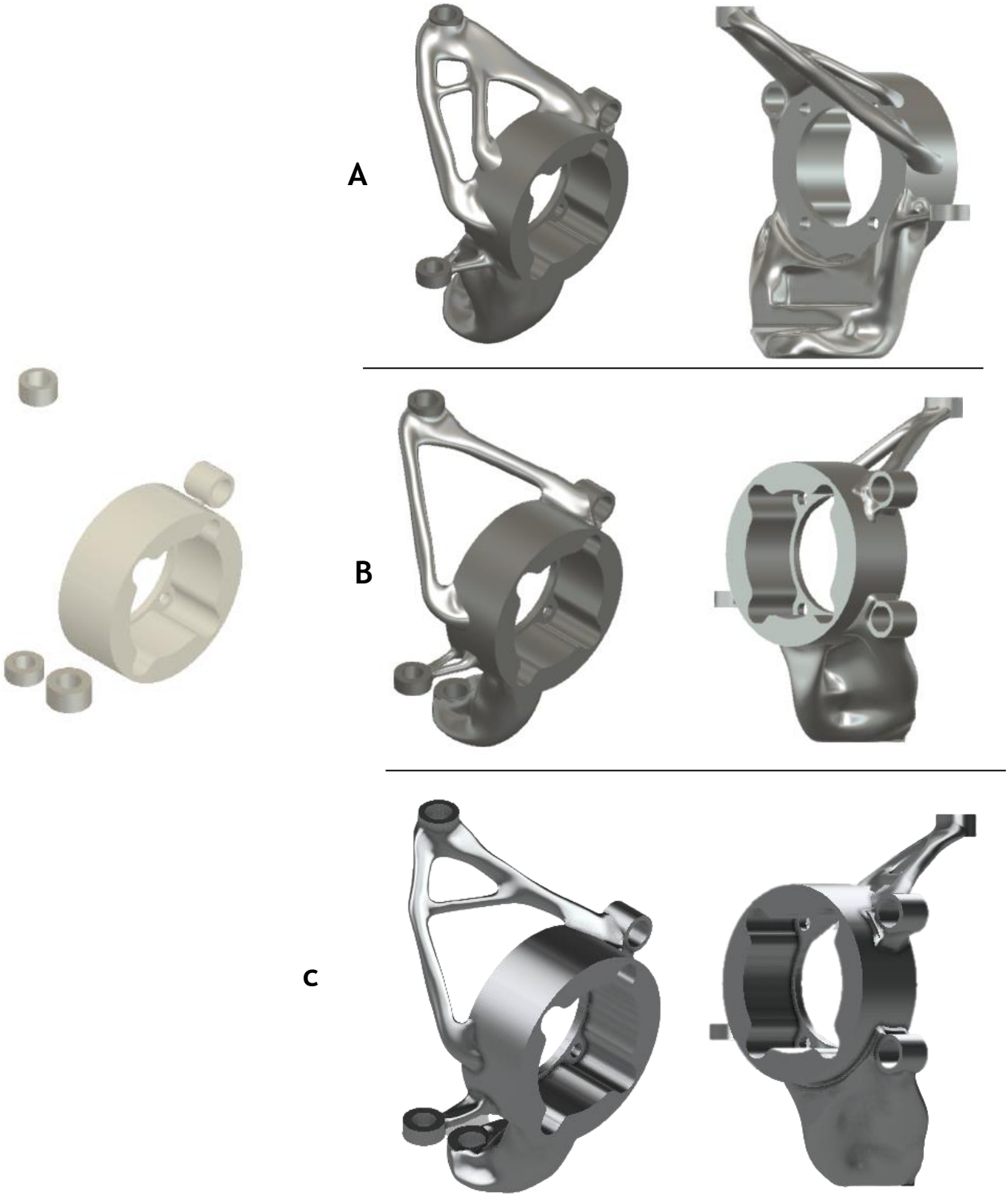


Figure 26 - S11

S12 differs from S11 in the diameter of the keypoints, to evaluate the dimension effect on the outcomes. As all previous simulations, the optimization occurred mainly in the top section. To evaluate if it was not generated any tension point, it was conducted a stress analysis, eliminating those concerns.

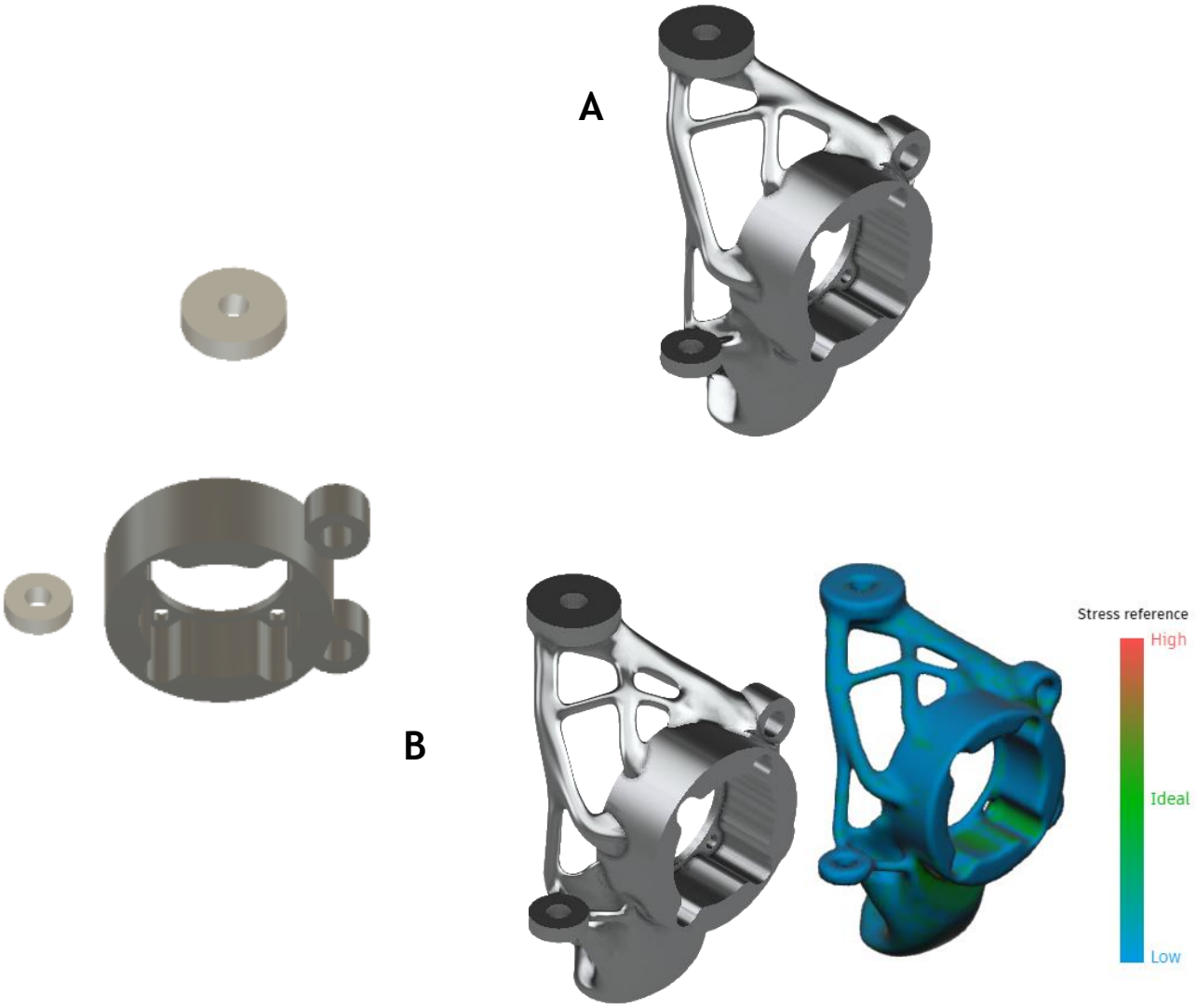


Figure 27 - S12

Additionally, it was also added to S13 that the obstacle corresponds to the caliper, and the width of the central body was reduced to evaluate the influence on the outcomes. As in the previous studies, when several constraints are selected, there is a region that is separated. Removing only one constraint, as in the other studies, creates viable results.

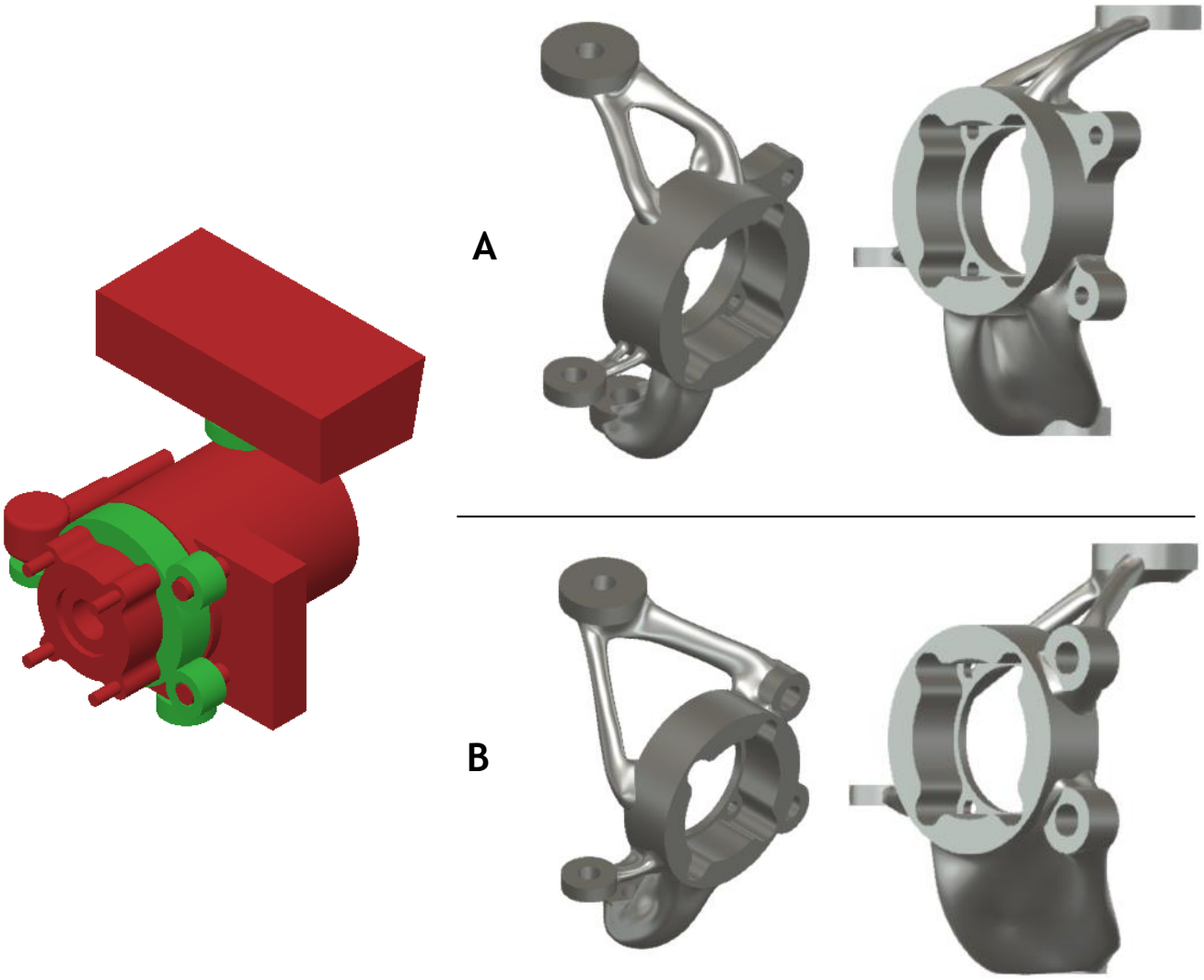
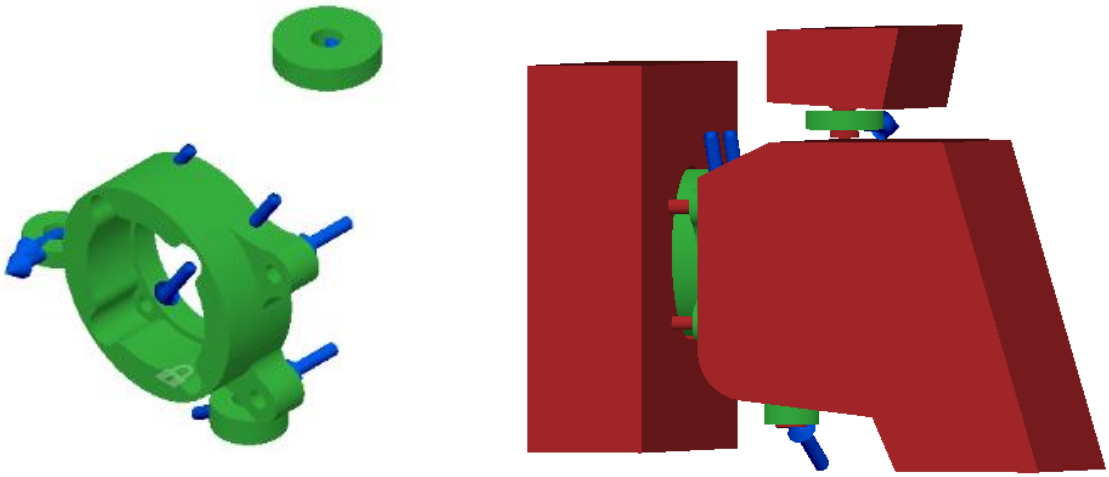
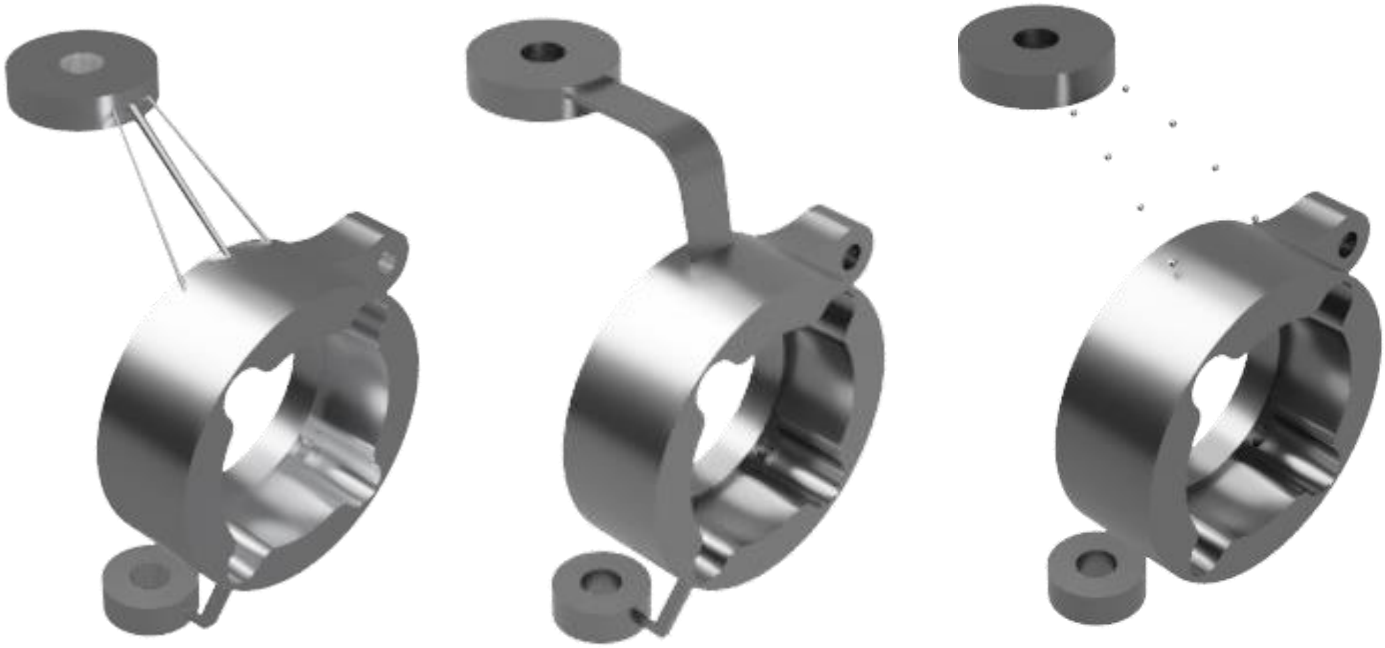


Figure 28 - S13

As demonstrated several times, the selection of several constraints negatively influences the generation of results, and to ease the solver, the obstacles were redesigned into a simpler and single body, where a new load case was applied. Alongside these changes, four simulations took place: S14, without any type of connection between the upper keypoint and the central body, and S15, S16, and S17, with three different approaches to connections. Each model was simulated twice, one identifying all keypoints as constraints,Figure 30, and the other considering only one constraint in the main body, Figures 31 and 32.

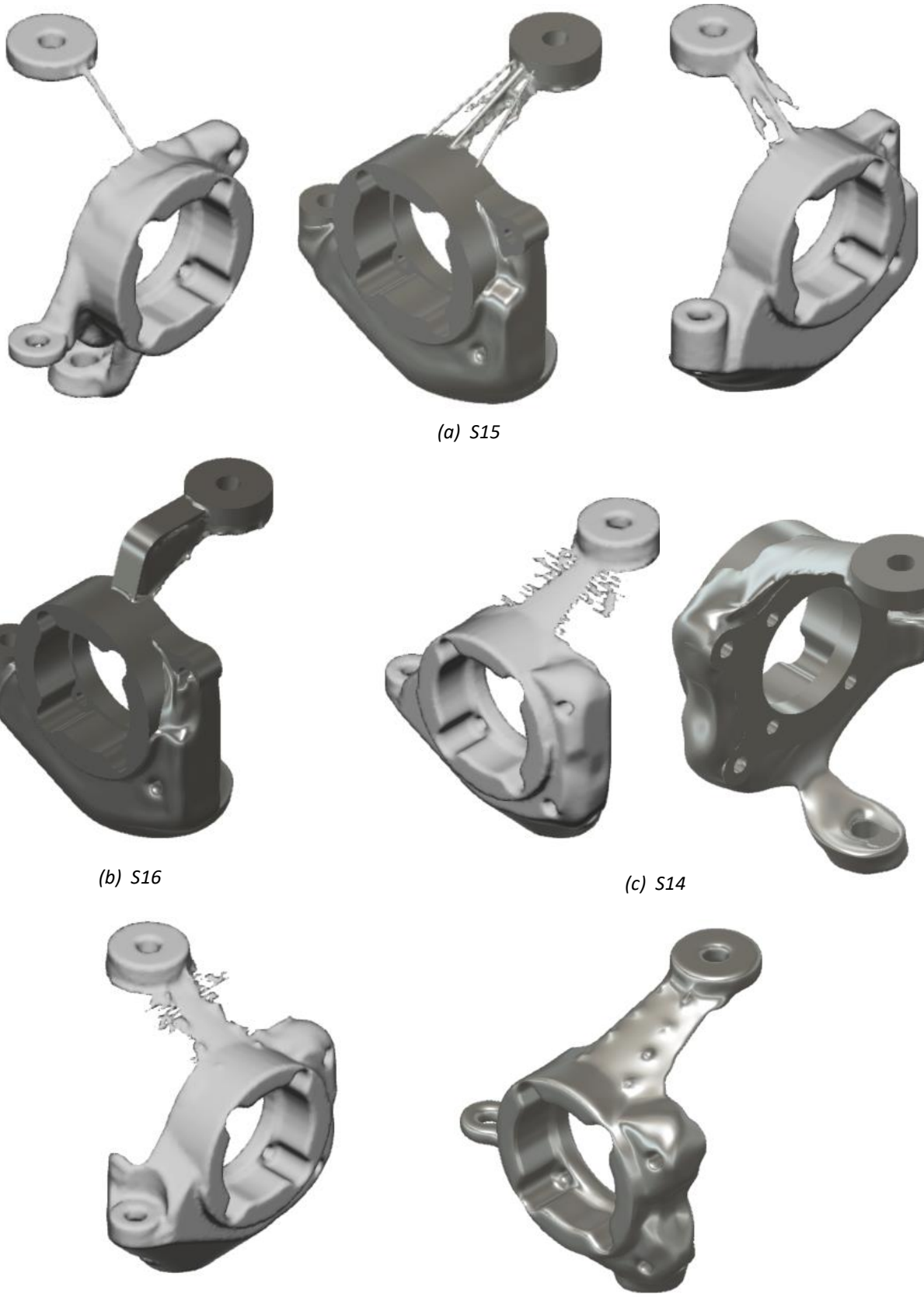


(a) S14 *(b) Obstacles*



(c) S15 *(d) S16* *(e) S17*

Figure 29 - Simulations S14 - S17



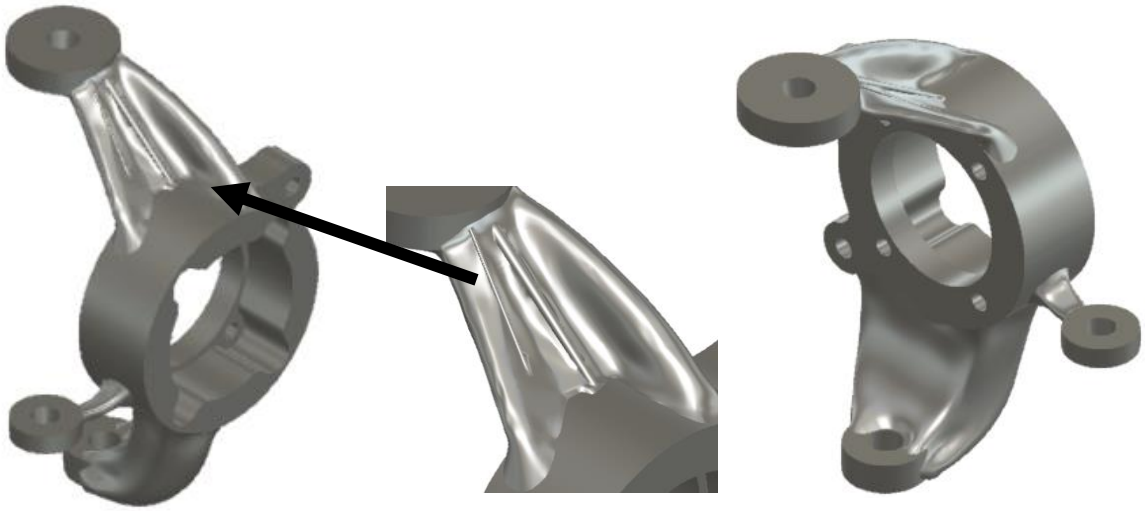
(a) S15

(b) S16

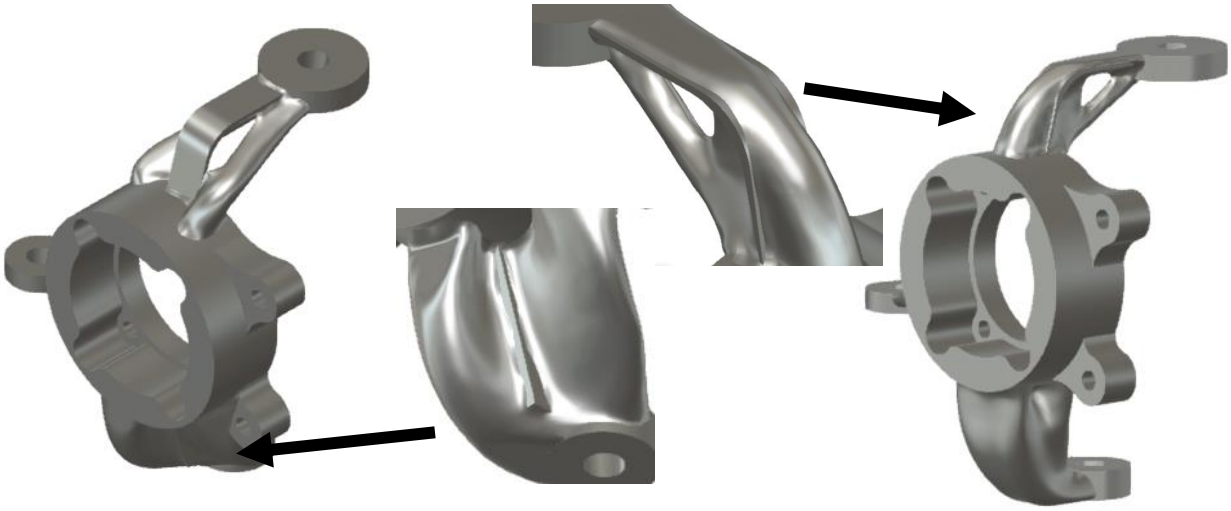
(c) S14

(d) S17

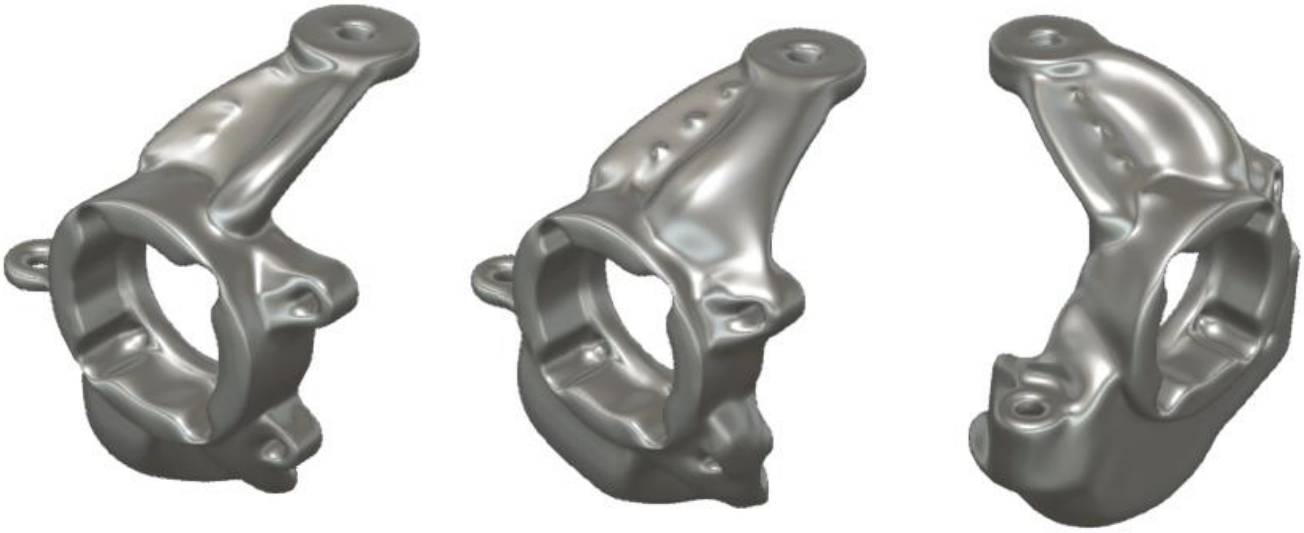
Figure 30 - S14 - S17 solutions when there are several constraints



(a) S15



(b) S16



(c) S17

Figure 31 - S15 - S17 solutions when there is only one constraint

A



B



C

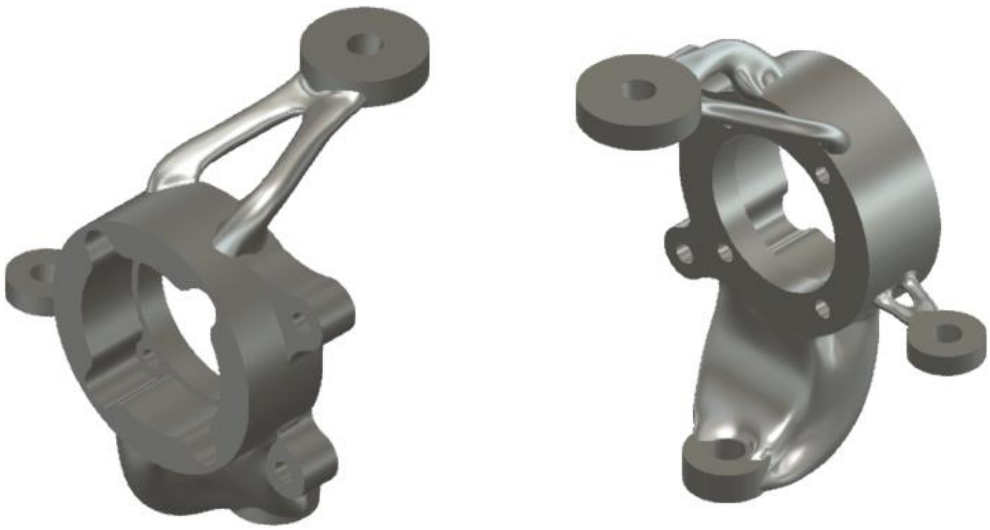


Figure 32 - S14 solutions when there is only one constraint

The impact of the number of constraints is evident when observing Figures 30 – 32. With the increase of the constraints, all the results labeled as "complete" displayed an error notice; however, a decrease to a single constraint in the main body significantly improves the quality of the generated results. Upon closer inspection of the highlighted sections, it becomes apparent that the given design was not fully integrated into the model. The results with higher quality for the second case load belong to Figure 32, S14 results when using only one constraint.

To address the limitation observed in the optimization of the lower section of all steering knuckles and to explore the solver's capacity, a new simulation, S18, was performed. This iteration utilized steel and iron as manufacturing materials. The results presented in Figure 33 demonstrate that the limitation is not regarding the selected material but the solver's capacity to generate results with this degree of complexity.



(a) Ductile Iron



(b) Cast Iron *(c) Steel*

Figure 33 - S18 results for a new list of materials

To summarize, all the decisions to apply each simulation are simplified in Table 6.

Table 6 - Summary of all simulations

Simulation	Differences from previous models	Reason	Problem
S2	Increase preserve bodies of S1	Indicate non-design geometries	Invalid results
S3	Redesign of obstacle bodies of S2	Correct obstacles geometry	Invalid results
S4	Remove initial body	Understand the influence of the addition of an initial body	Invalid results
S5	Redesign of obstacle bodies of S4	Simplify obstacles to achieve better results	Invalid results
S6	Redesign the initial body to a box-shaped geometry	Understand the influence of the initial body on the generated models	Did not take into consideration the movement of the lower control arms
S7	Application of loads on the caliper connection	Generate connections between the key points and the central body	Connection was not generated
S8 - S9	Addition of a physical connection between the keypoints and the central body	Generate connection between the keypoints and the central body.	Invalid results
S10	Correction of assembly position and addition of an obstacle to represent the movement of the lower control arm	Correct geometry mistakes	Invalid results when several constraints were applied
S11	Increase in wall thickness	Understand the influence of the wall thickness in the generated models	Low grade of optimization of lower section
S12	Increase diameter on upper keypoint	Understand its influence on the generated models	Low grade of optimization of lower section
S13	Addition of the calliper obstacle	Correct geometry mistakes	Low grade of optimization of lower section
S14	Application of a new load case and simplification of obstacles	Understand its influence on the generated models	Invalid results when several constraints were applied
S15 - S17	Introduction of geometries to simulate connection with the central body	Generate connections between the key points and the central body.	Invalid results when several constraints were applied

5.2.3. Designs created by Sheet Metal Function

The literature survey was also fundamental to understanding that there is no specific geometry to follow as long as the mechanical requirements and key points are met. Therefore, in the sheet metal function, a new model was created.

As the tie rod connection is on a different plan, it will restrict the construction of the model. There are several approaches to creating the model; one is to design the "main" body by sheet metal function and the tie rod connection section separately and connect both by a welding process. Although most of the selected materials are suitable for welding, the software, at present, is not capable of performing simulations with welded joints, preventing the study of the viability of the structure. The approach used consisted of creating a single model for two rounds of sheet metal with a spacing between the "main" body and the connection, as shown in the following Figure.

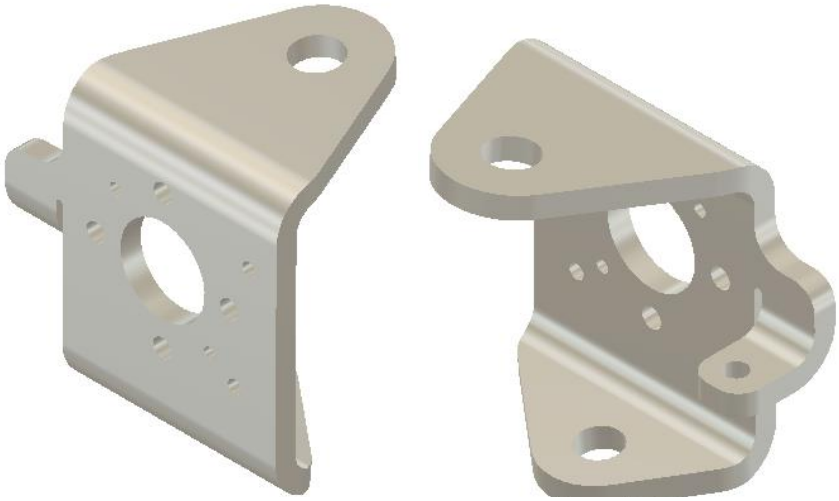


Figure 34 - Steering Knuckle geometry created for sheet metal forming

It was simulated in two models, only differing on the thickness, being 15 mm in one and 19.5 mm in the other. The k value (the ratio of the neutral axis to the material thickness) was kept constant. The simulations were conducted using the second set of load cases, and the results of the simulations are displayed in Table 7 and Figure 35.

Table 7 - Simulation results

		FoS		**Stress**		**Displacement**	
		min	max	min	max	min	max
A (15 mm)	FWOB	4.414	15	0.05753	90.61	0	0.4396
	CURB	5.398	15	0.049388	74.08	0	0.682
	RB	10.91	15	0.02271	36.65	0	0.1781
B (19.5 mm)	FWOB	6.948	15	0.04678	57.55	0	0.2404
	CURB	3.307	15	0.2116	120.9	0	0.4349
	RB	15	15	0.04546	20.6	0	0.09541

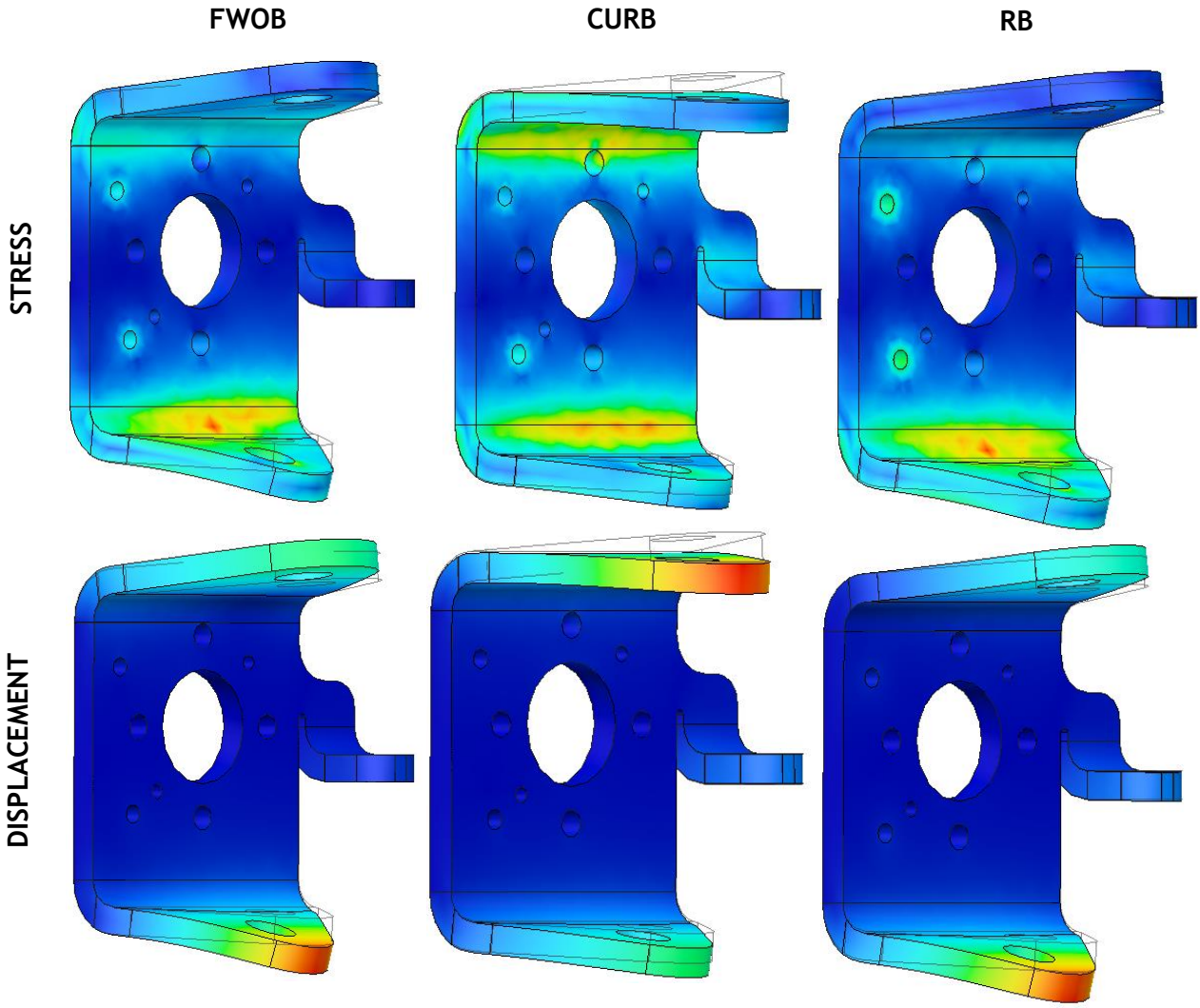


Figure 35 - Results of the simulation of sheet metal model

The tensions are mostly located on the flexing areas, while the displacement is detected on the lower section for the FWOB and RB and the upper section for the CURB. As mentioned before, these results have an adjusted deformation of 5% to have a visible dislocation, but the maximum displacement present is lower than 0.7 mm.

These could be selected as viable solutions; however, since the main purpose of this thesis is to achieve design optimization and an original design, this approach is not ideal.

5.3. Control arm

5.3.1. First Geometry

Similarly, for the steering knuckle, a first simulation was conducted on the given model of the control arm.

Ideally, the constraints were located exactly where the loads were applied to guarantee that the assembly scheme was kept in place. However, that is not possible, so

the best compromise was to only select the inside of the joint and the outside diameter of both bushes since their displacement is almost zero. In the Figure, it is possible to observe the displacement that takes place in the joint if the interior diameter is not selected. As the other component, the materials in the study are A356 T6 and 2014 T6, and the results are presented in the following Table.

Contrary to the Steering knuckle, when there are three constraints, the factor of safety is over the expected, making it a viable model; however, when only selecting the joint as a constraint, the value decreases to values under 0.

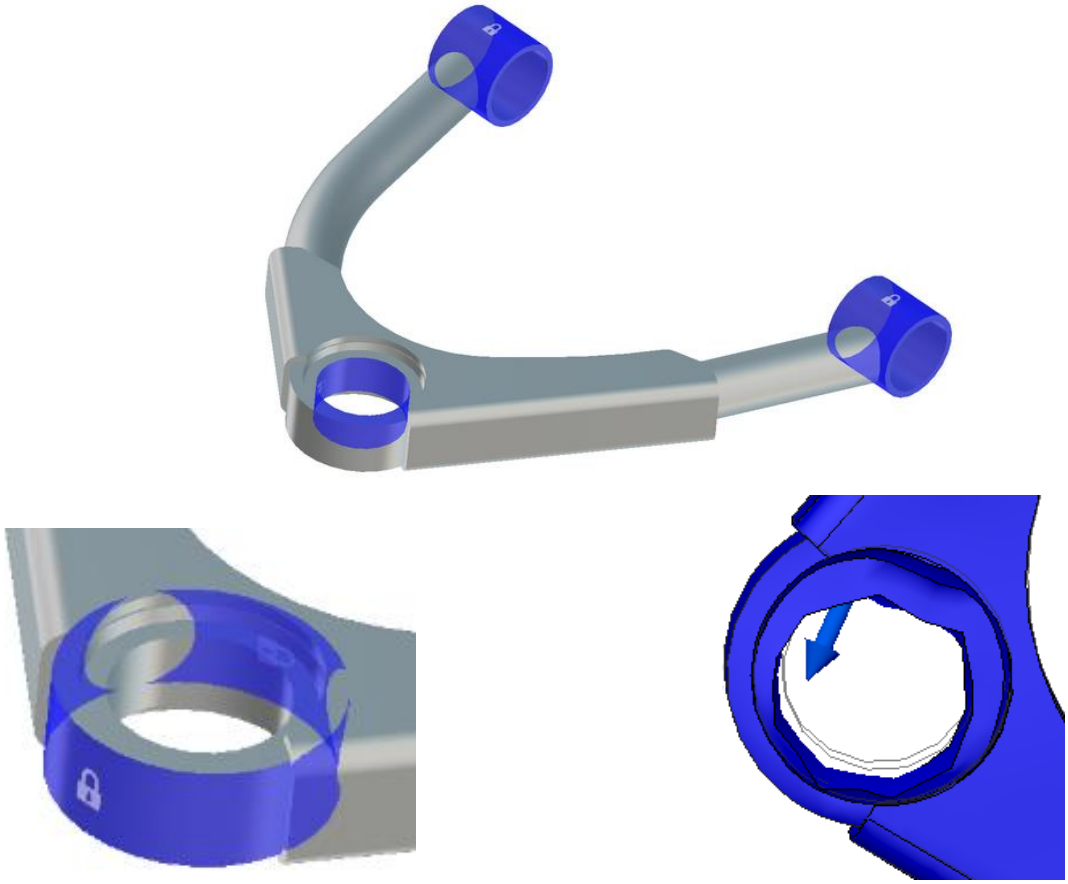
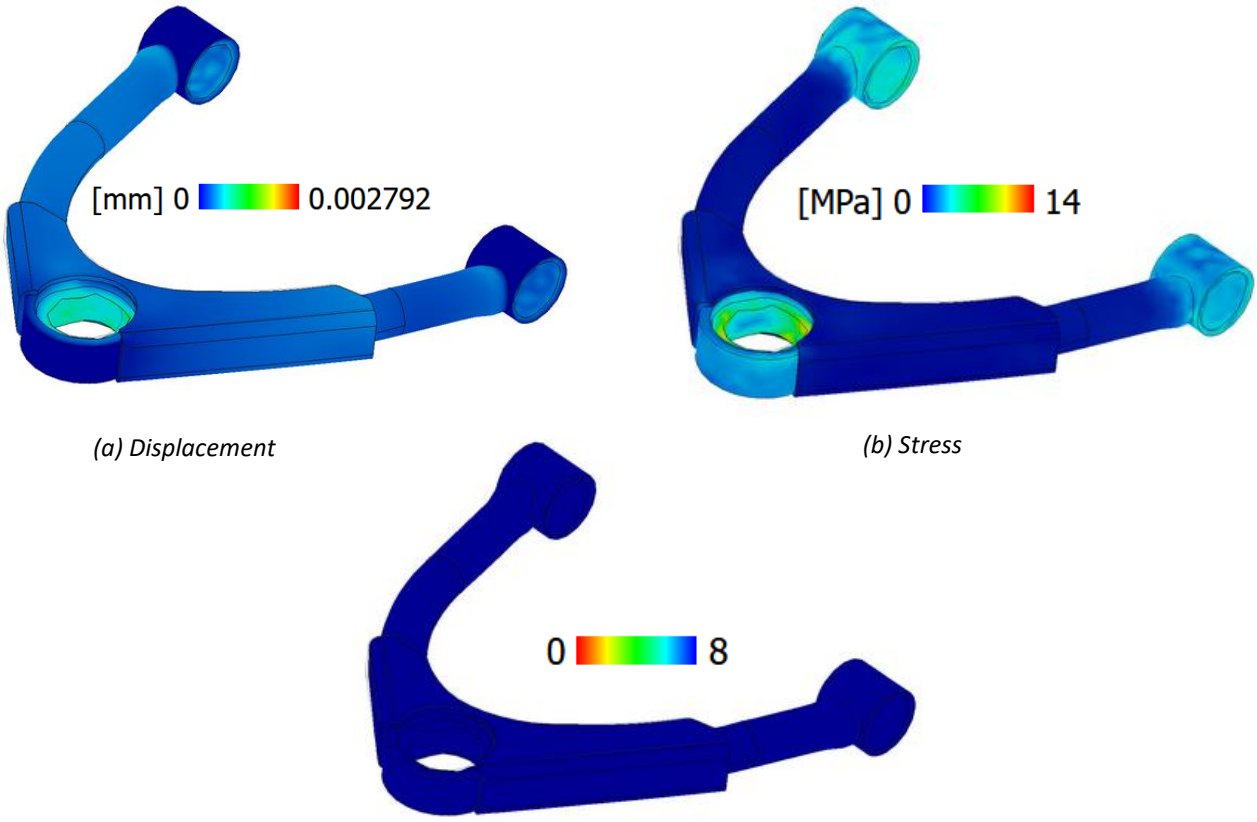


Figure 36 - Control Arm's constraints for initial simulation

Table 8 - Simulation Results

	Factor of Safety			**Stress (MPa)**				**Displacement (mm)**	
	min		max	min		max		min	max
	A356 T6	2014 T6		A356 T6	2014 T6	A356 T6	2014 T6		
FWOB	13.47	15	15	1.566e-6		12.25		0	0.002922
CURB	10.52	15	15	5.624e-4		15.69		0	0.00157
PB	11.78	15	15	3.289e-4	2.983e-6	14	11.31	0	0.002791

FWOB – Front wheel overbump | CURB – Lateral Curve Strike | PB – Panic break



(a) Displacement

(b) Stress

(c) FoS

Figure 37- Results of the simulation on the initial geometry

5.3.2. Designs created by Generative Design

Being a simpler component than the Steering Knuckle, the learning curve of the assembly and obstacles is slimmer, with fewer errors detected in the assembly of the models; however, the try-and-error method also took place in these simulations.

The constraints used were the following:

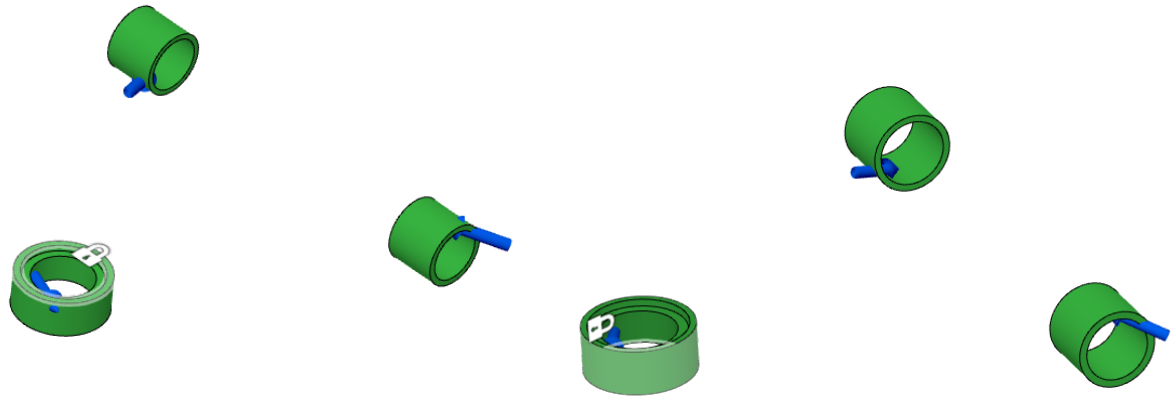


Figure 38 - Constraints used during Control arm's simulations

The cylindric part of the given model was allowed since this component is not subjected to a high number of loads and to keep the weight low.

In the initial idea of welding the created bushes and joints to the created "cylinders", the original connection to the keypoints was kept to indicate to the solver to keep the geometry. As pointed out in detail in the Figure, the solver did not take into consideration the connection, excluding this simulation.

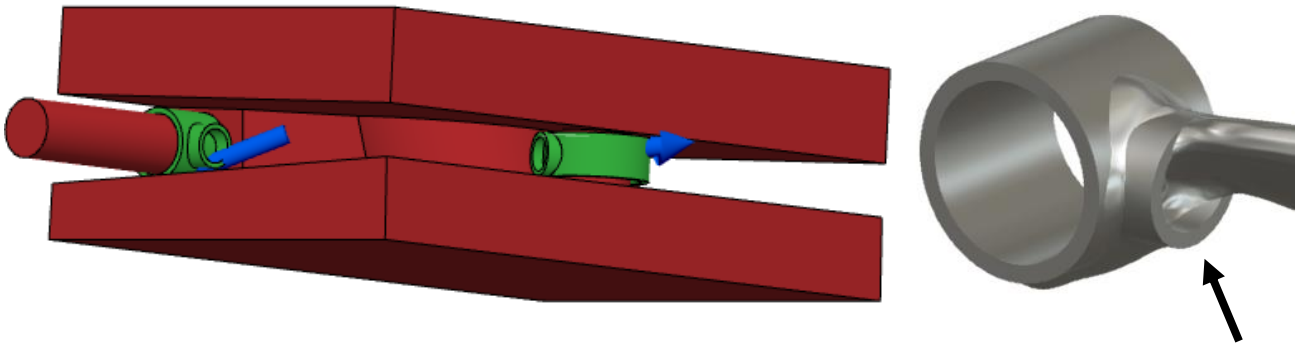


Figure 39 - S1 (Control Arm), conditions on the left and result, on the right

At the time of the elaboration of this thesis, Fusion 360 did not own a solver for welding joints, so the idea of S1 was excluded. S2 was then created with a slight increase in obstacles and, although eliminating the initial connection, cuts were created in the obstacles to indicate the connecting area.

Some of the outcomes generated increased the mass, not achieving the goal of topological optimization. However, the simplification of the geometry and the loads in relation to the other components generates greater results.

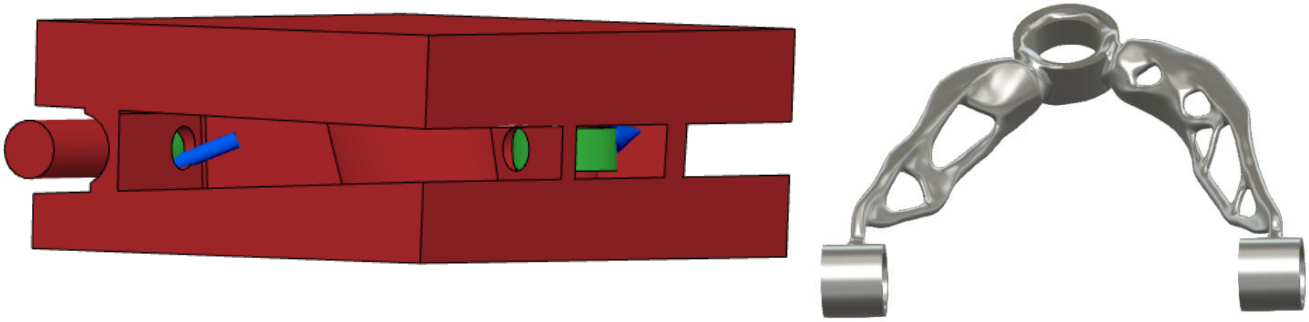


Figure 40 - S2 (Control Arm)

S3 added the initial body to the obstacles designed in S2 to indicate to the solver the path the design should take. However, as it is possible to see in Figure 41, the results were not valid. The connection with the joints is severely affected by the obstacle geometry, requiring an alteration in future simulations.

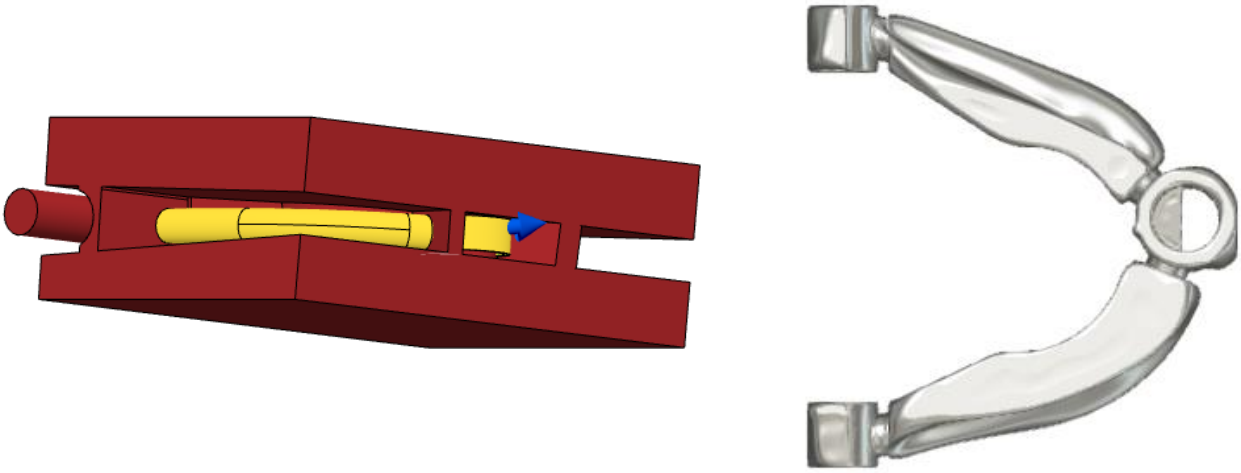


Figure 41 - S3 (Control Arm)

Two more models were designed with a higher amount of obstacles to understand its influence in the results.

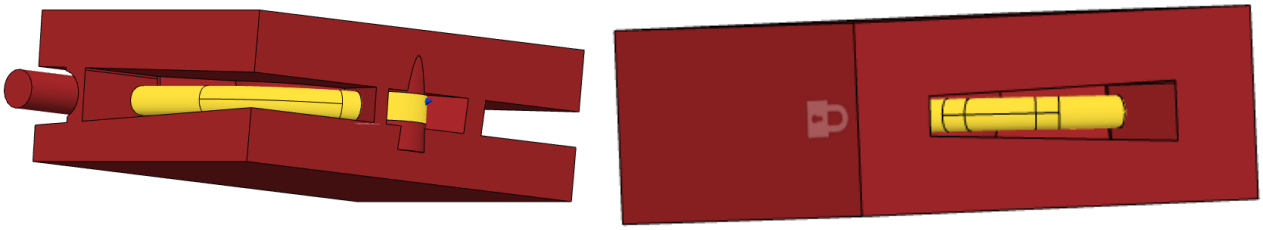


Figure 42 - S4 and S5 (Control Arm)

As proved in the Steering Knuckle, when under restrict conditions and inputs, the solver tends to generate weaker results. In both simulations there was an error notice in all results, indicating Fusion encountered a problem and could not carry on the simulation.

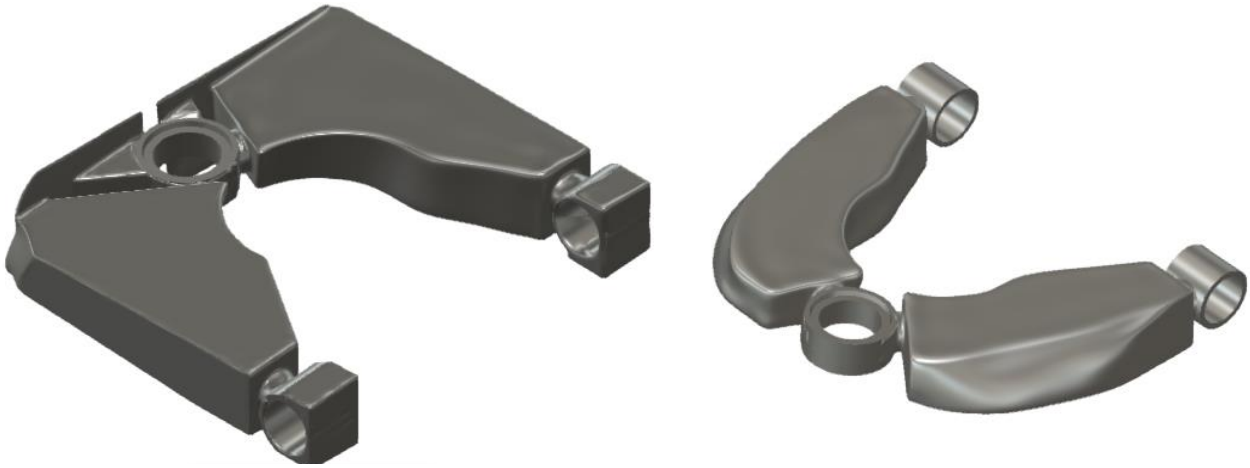


Figure 43 - S4 and S5 example results

To understand if a simplification would generate valid results, S6 was created, keeping all the main restrictions except for the height limitation.

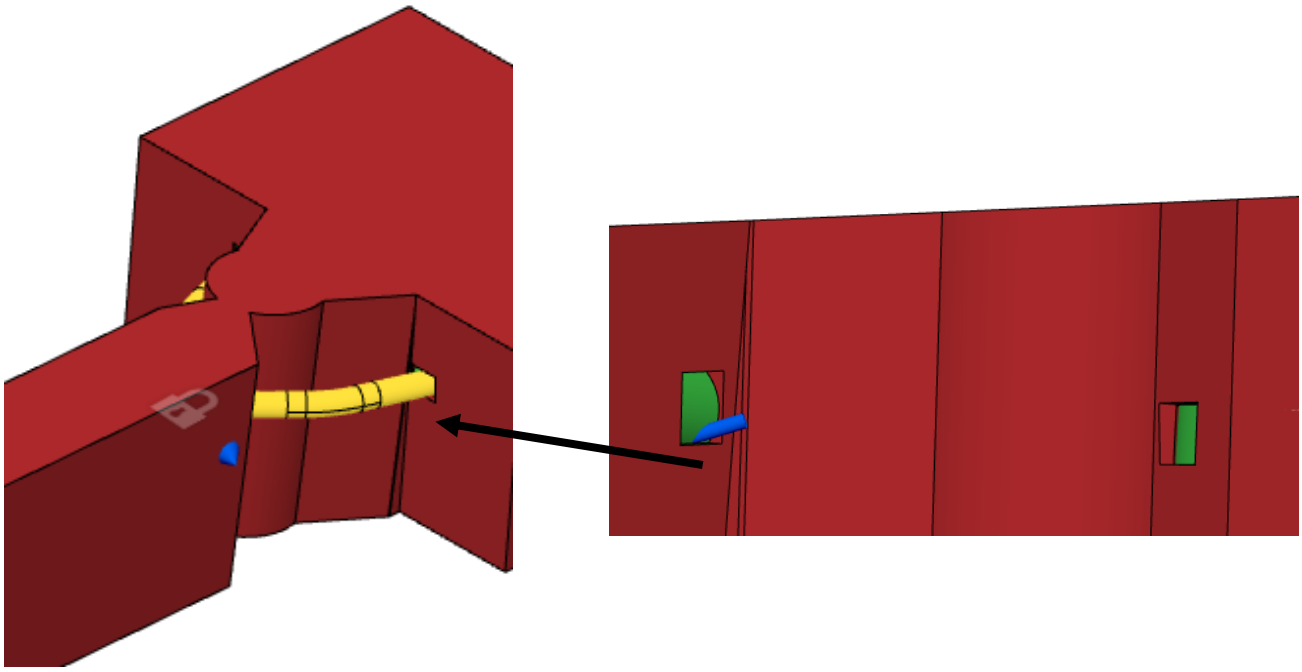
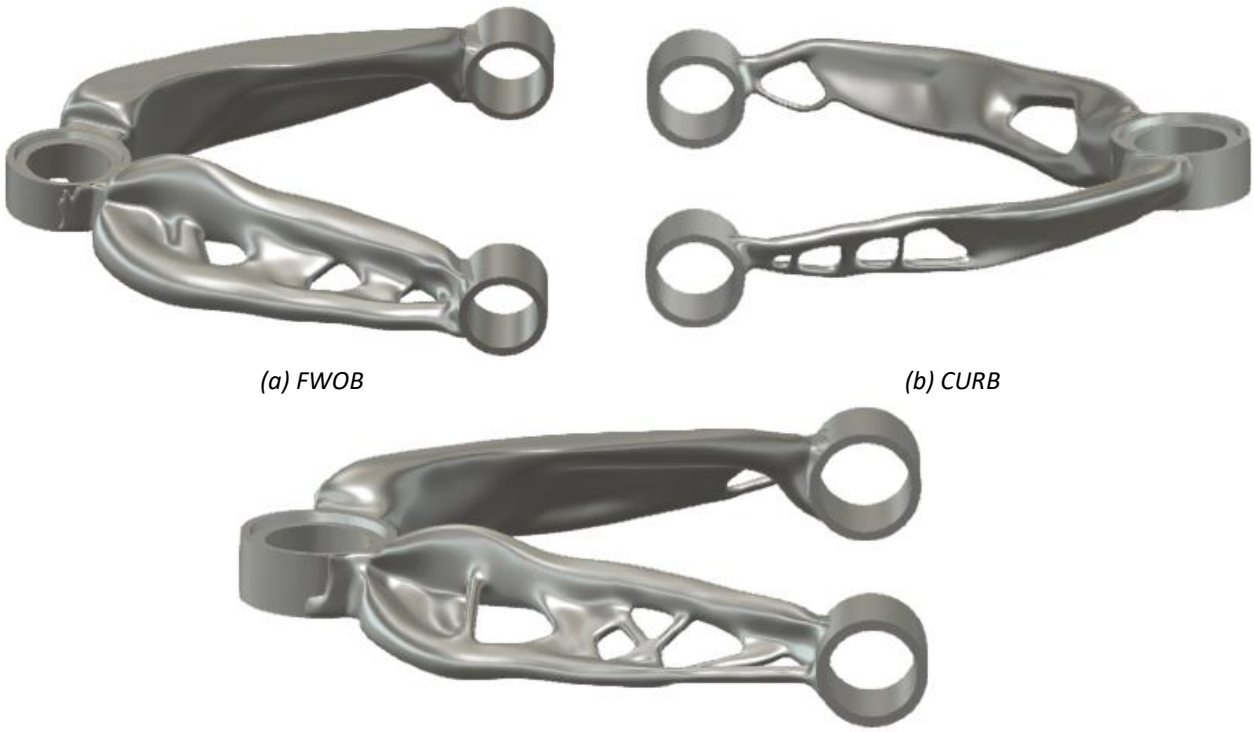


Figure 44 - S6 (Control Arm)



(a) FWOB *(b) CURB*

(c) PB

Figure 45 - S6 (Control Arm) Results

Although the previous simulation already generated valid results, they were very restricted in the connections with the bushes and the joint, so, for S7, the “openings” for these connections were increased.

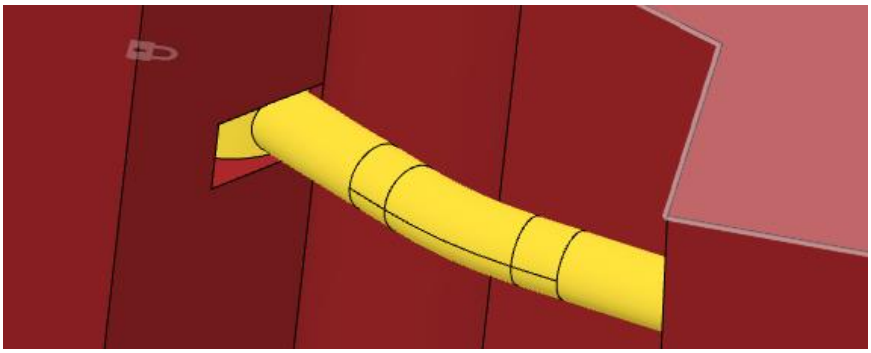


Figure 46 - S7 (Control Arm)

This model had valid results in all three simulations, therefore there were not conducted more simulations regarding this components.

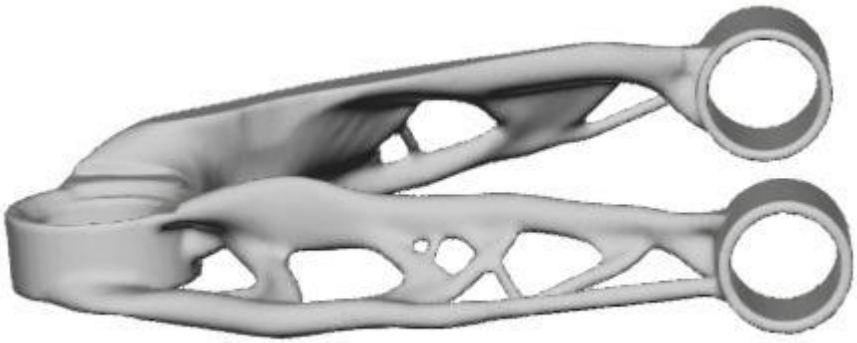
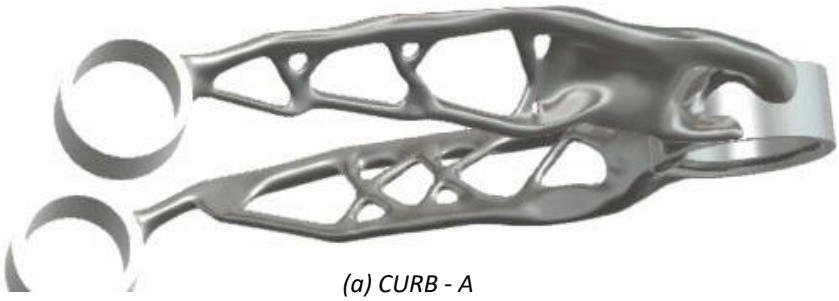


Figure 47 - S7 (Control Arm) FWOB result



Figure 48 - S7 (Control Arm) PB result



(a) CURB - A



(b) CURB - B

Figure 49 - S7 (Control Arm) CURB results

6. Result analyzis

Through the simulations, it was possible to withdraw some considerations regarding the software. There were several error notes through all the simulations, as represented in Figure 50 and Figure 51. In the research done in Granta, of all the materials studied, only A356 and AlSi10Mg are suitable for casting; however, Fusion also created results for all the materials as die casting. Also, for several materials, for example, alloy 7075 and 7050, the software could not compute any simulation. As mentioned previously, the die casting process is still in development, and, as it is possible to see in Figure 50, there was no viable result.

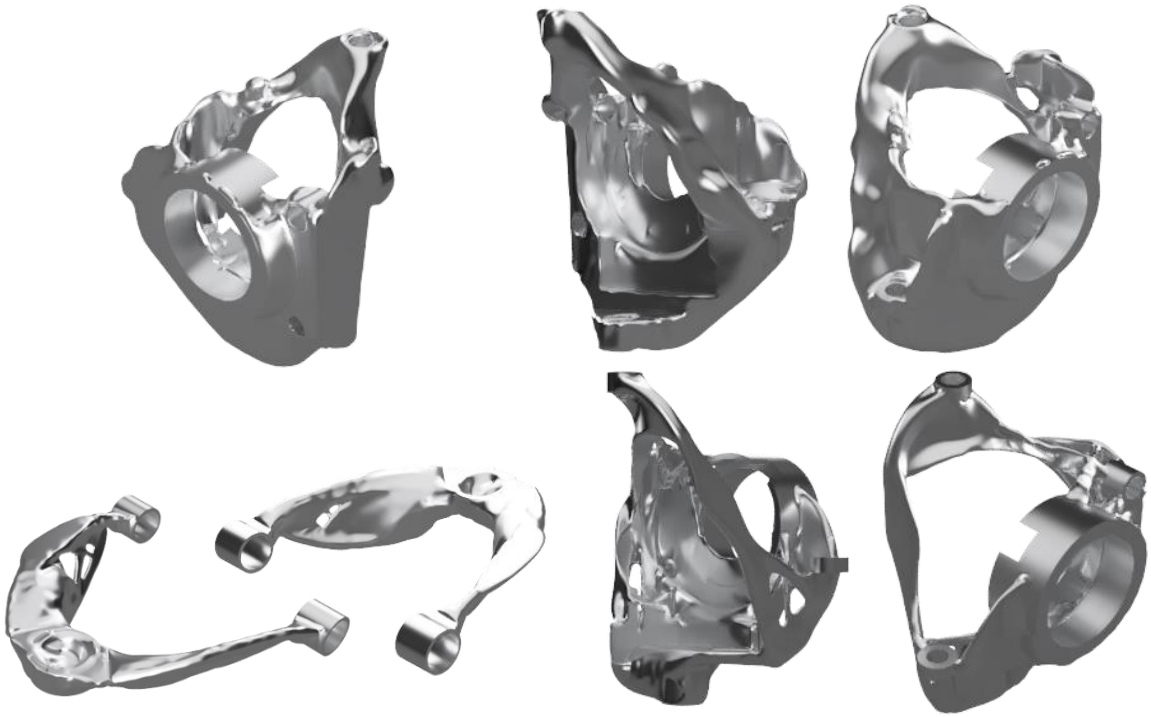


Figure 50 - Die Casting Results

Each component was subjected to three individual simulations according to the load cases and inputs mentioned before, creating separate results for each load case. Ideally, a component would present a geometry capable of withstand all the load cases; however, since they were applied individually, the chosen model will not be the best in all cases. Therefore, it is required that, after selecting the model, simulating it for the other two load cases be done to see if it is a viable solution.

Along the way, especially in the steering knuckle, with an increase in the constraints, there is a decrease in the viability of the design of the models.

Although some simulations generated interesting results, most of them were invalid, with error notices as follows:



Figure 51 - Error Notices

6.1. Steering knuckle

The following Table presents the best results. To note that these results are retrieve directly from Generative Design and were not optimized. The initial mass, of the steering knuckle made of A356 T6 was 1528.997 g.

Table 9 - Best results comparison – Steering Knuckle

Study	Material	Manufacturing method	Volume	FoS	Mass (Kg)	Stress (Mpa)	Max Displacement (mm)	% Weight reduction
S11 A	A356T6	unrestricted	559288.277	2	1.493	82.5	0.398	2.29
S11 B	6061	unrestricted	377795.36	2	1.02	137.5	0.712	33.25
S11 C	6061	AM	389445.96	2	1.052	137.5	0.718	31.15
S12 A	6061	unrestricted	557338.967	2	1.505	95.802	0.456	1.51
S12 B	A356T6	unrestricted	620480.036	2	1.657	82.5	0.372	-8.44
S13 A	A356T6	unrestricted	412040	2	1.1	82.5	0.251	28.01
S13 B	A356T6	AM	439922.892	2	1.175	82.5	0.249	23.10
S14 A	2014 T6	AM	406227.956	2	1.133	199.95	0.745	25.9
S14 B	2014 T6	unrestricted	396733.734	2	1.107	199.95	1.072	27.6
S14 C	2014 T6	unrestricted	377985.326	2	1.054	199.95	0.792	30.6

It is possible to observe that most of the valid results were produced by an unrestricted method, or AM, making it impossible to calculate the unitary cost for the unrestricted results. Regarding the displacement, the better geometries are S13 A and B, while also maintaining a high percentage of weight reduction. The results with better mass optimization are S11 B and C; however, their displacement and stress are the highest. Regarding the mass, there is no significant distinction between the mentioned results.

The models need to be optimized (cylindrify and smooth surfaces), possibly changing these properties, and tested for the remaining two load cases to understand if they are a viable solution for all cases.

S14 results were simulated with different load cases from the other models; therefore, a comparison with all the results is not the most viable. Although their weight reduction is significant, the stress and displacement values are the highest of all the results mentioned.

With these results, setting aside S14 results, the best models to choose are S13 A and B.

As mentioned in this document, there was a significant disparity between the optimization between the top and bottom sections of the steering knuckle, which leads to the understanding that, even though it created partially interesting results, the solver is still not powerful enough to simulate models with this high grade of complexity.

6.2. Control arm

The following Table presents the best results between all control arms simulations. To note that these results are retrieved directly from Generative Design and were not optimized. The initial mass, of the control arm made of A356 T6 was 546 g.

Table 10 - Best results comparison – Control Arm

	Material	Manufacturing method	Volume	FoS	Mass (Kg)	Stress (Mpa)	Max Displacement (mm)	%weight reduction
FWOB	2014 T6	unrestricted	191406.4	1.793	0.534	223.085	5.592	2.20
CURB A	2014 T6	unrestricted	131577.7	2	0.367	199.947	7.324	32.78
CURB B	6061	unrestricted	157419.3	2	0.425	137.5	4.464	22.16
PB	2014 T6	unrestricted	175635	1.791	0.49	223.31	6.057	10.26

It is possible to observe that most of the results are made of 2014 T6 by unrestricted methods. Both results for FOWB and PB in the connection regions, Figure 52, presented a FoS lower than 2, needing to be optimized to see if these values can achieve the required value of 2. The displacement values are also elevated, as shown in Figure 53, because they are located on the bush. To understand if these displacements would affect the suspension's safety, further simulations of the entire assembly should be made, however, the entire load cases was not provided to perform the simulations.

Another approach to try to avoid this error was to utilize, as the initial model, a reinforcement, in the connections areas.

Taking into consideration the present results and assuming the displacement does not have a negative impact on the assembly, it should be selected a geometry between the CURB results since they are the ones with higher mass reduction and less stress.

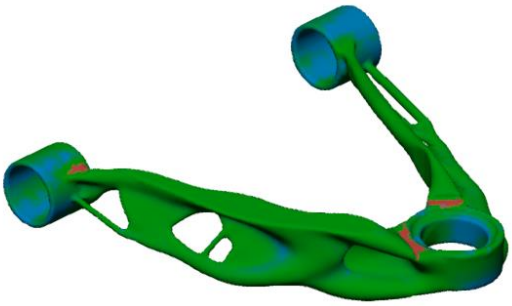


Figure 52 - FoS Analysis

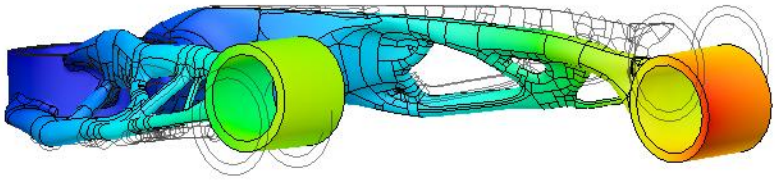


Figure 53 - Displacement Analysis

7. Conclusion

In theory, Generative Design holds immense potential for creating several innovative geometries based on the same inputs. This function allows engineers to create unique models in a reduced amount of time.

This work took place between the months of March and June 2023, therefore, all the results generated are correspondent to the update of fusion available in that timeframe. However, it should be noted that these results may become outdated with further software updates.

Regarding the generated models, it can be observed that while there was significant topological optimization in the upper section of the steering knuckle, the solver was unable to complete the same grade of optimization in the lower section. Nonetheless, even with this limitation, the models achieved a mass optimization of over 30%.

For the control arms, despite setting a minimum required factor of safety (FoS) of 2, there were simulations where this criterion was not met, simultaneously a high displacement was detected.

In both simulations it was detected that the increase of the level of detail in the obstacles and constraints led to weaker or even invalid results, raising concerns about the solver's capacity to generate components with a high degree of complexity.

Although the ideal results were not attained, the software exhibits great potential. While there are other software options available for topological optimization, such as nTopology, most of them have steeper learning curves and do not offer the same level of flexibility as Fusion in terms of incorporating inputs.

At present, Fusion falls short of fully delivering on its promises when subjected to high loads and numerous restrictions. It is hoped that Autodesk will update the solver in the future, enabling this method to fulfill its purpose and assist engineers in creating faster and more innovative models.

Bibliography

[1] Heißing, B., Ersoy, M. 2016. Chassis Handbook: Fundamentals, Driving Dynamics, Components, Mechatronics, Perspectives. Wiesbaden: Vieweg+Teubner.

[2] Mallick, P. K. (2010). Materials, Design and Manufacturing for Lightweight Vehicles - 1.1 Introduction. Woodhead Publishing.

[3] Gysen, B.L.J. & Paulides, Johannes & Lomonova, E.A. 2011. Generalized Harmonic Modeling Technique for 2D Electromagnetic Problems Applied to the Design of a Direct-Drive Active Suspension System.

[4] Student Lesson. April 4th 2022. "Different Types of Suspension System and Their Functions - Studentlesson." Accessed on March 8th, 2023 https://studentlesson.com/types-of-suspension-system/.

[5] Team, Wuling Tech. 2021. "8 Types of Car Suspensions." Wuling. Accessed on March 8th, 2023 https://wuling.id/en/blog/autotips/8-types-of-car-suspensions.

[6] Spinny Blog. "Types of Suspensions | Spinny Blog." 2021. Accessed on March 8th, 2023. https://www.spinny.com/blog/index.php/types-of-suspensions/.

[7] Digit Insurance. "Types of Suspension Systems: How They Worked & Parts of Car Suspension." Accessed on March 8th, 2023 https://www.godigit.com/motor-insurance/car-insurance/car-parts/types-of-suspension-systems.

[8] Hagroo, Shashi. 2019. "FEA of Double Wishbone Suspension System Under Extreme Driving Conditions".

[9] Simionescu, Petru & Beale, David. 2002." Synthesis and analysis of the five-link rear suspension system used in automobiles". Mechanism and Machine Theory - MECH MACH THEOR.

[10] Hasan, Shahriar & Ahmed, Ashfaq & Ahmed, Nihal & Mamun, Muntasir. 2021. "A Finite Element Analysis of Automobile Leaf Spring".

[11] Macfarlane, Alexander. 2016. "Modular Electric Automatic Guided Vehicle Suspension-Drive Unit".

[12] Jörnsen Reimpell, Helmut Stoll, and Jürgen W Betzler. 2001. "Types of

Suspension and Drive". pages 1–85.

[13] Mirzana, Ishrat, and Syeda Begum. 2018." Review of MATERIAL OPTIMIZATION of STEERING KNUCKLE for LOW SPEED VEHICLE". Journal of Emerging Technologies and Innovative Research

[14] Srinivasan, Athi. 2019. "Review of Design and Optimization of an Off-Road Mini Baja Steering Knuckle".

[15] Deshpande, Aditya & Ekabote, Nagaraj & Sridhar, A & Vernekar, Akshay. 2020. "Design cycle implementation on a customized steering knuckle for a competition ATV". Journal of Physics: Conference Series.

[16] Krishna Teja, Nittala & Teja, Avrk & Harsha, J.Sri. 2016. "Design and Manufacturing of Knuckle for an Electric All-Terrain Vehicle". Imperial Journal of interdisciplinary Research.

[17] Kamble, Ankur. 2017. "Review of Developmental Design and Optimization of Steering Knuckle with Integrated Spindle". IJSRD - International Journal for Scientific Research & Development

[18] Yadav, Sanjay. 2016. "Review of Design and Analysis of Steering Knuckle Component". International Journal of Engineering Research & Technology

[19] Jeon, Gyu, Ki Kim, Jung-Hwa Moon, Chul Lee, Whi-Jun Kim, and Suk Kim. 2018. "Effect of al 6061 Alloy Compositions on Mechanical Properties of the Automotive Steering Knuckle Made by Novel Casting Process." Metals 8.

[20] Patil, Gopal. 2016. Review of Evaluation and Optimization of Macpherson Steering Knuckle Using Topological Approach. International Journal of Engineering Research & Technology (IJERT) 5 (3). issn: 2278-0181.

[21] SECO. 2014. "Proven solutions for steering knuckle [review of proven solutions for steering knuckle]".

[22] Triantafyllidis, G. K., A. Antonopoulos, A. Spiliotis, S. Fedonos, and D. Repanis. 2009. "Fracture Characteristics of Fatigue Failure of a Vehicle's Ductile Iron Steering Knuckle." Journal of Failure Analysis and Prevention 9.

[23] Tigges, Rolf D. 2000. "Review of EUROPEAN PATENT APPLICATION", issued 2000.

[24] Cole, Greg M. 2001. "Automotive Chassis/Suspension Materials".

[25] Lampman, S. 2018. “Permanent Mold Casting of Aluminum Alloys.” Aluminum Science and Technology.

[26] B.Babu, M. Prabhu, P.Dharmaraj, R. Sampath. 2014. “Stress analysis on steering knuckle of the automobile steering system”. IJRET: International Journal of Research in Engineering and Technology, volume 3, issue 3.

[27] Bagus Aulia Saputro, Ubaidillah, Dicky Agus Triono, Dzaky Roja Pratama, Sukmaji Indro Cahyono, Fitrian Imaduddin. 2018. “Static load simulation of steering knuckle for a formula student race car”. AIP Conference Proceedings.

[28] Subaru Parts Plus. “What Is a Steering Knuckle and Why Is It Important?”. Accessed on March 8th, 2023.
https://www.subarupartsplus.com/blog/steering-knuckle-explained.

[29] “Steering Knuckle Market: Global Industry Analysis and Forecast (2022-2029) by Vehicle Type, Manufacturing Method, Material Type and Region.” n.d. MAXIMIZE MARKET RESEARCH. Accessed March 23rd, 2023.
http://www.maximizemarketresearch.com/market-report/global-steering-knuckle-market/70901/.

[30] Mallick, P.K. 2021. “Overview.” Materials, Design and Manufacturing for Lightweight Vehicles, 1–36.

[31] Davis, J R. 2001. Alloying: Understanding the Basics. Materials Park, Oh: Asm International.

[32] Choksey, Jessica. 2021. Review of What Is a Control Arm on a Car? Edited by J.D.Power. J.D.Power. January 8, 2021. Accessed on March 8th, 2023.
https://www.jdpower.com/cars/shopping-guides/what-is-a-control-arm-on-a-car.

[33] “What Do Control Arms Do? Upper & Lower Control Arms - 1A Auto.” Accessed on June 8th, 2023.
https://www.1aauto.com/content/articles/control-arms.

[34] R., Jhala. 2010. “Review of Geometry and Size Optimization for a Steering Knuckle with No Change in Attachment Geometry by Reducing Production Cost and Weight”. International Journal of Advanced Engineering & Application.

[35] Martinez, Yobani. 2017. “Review of design optimization of race car steering knuckle for additive manufacturing”. Master’s thesis, University of Texas at Arlington.

[36] Borsato, Gabriele. 2020. “Review of Design of a Maraging Steel Steering Knuckle for Additive Manufacturing”. Master’s Thesis, Politecnico di Torino.

[37] Petr, Tomas. 2020. “Review of DESIGN and OPTIMIZATION of the STEERING KNUCKLE for an UTILITY VEHICLE”. In INEGI-FEUP.

[38] Jasoliya, Dhruvin, Dhaval B. Shah, and Absar M. Lakdawala. 2022. “Topological Optimization of Wheel Assembly Components for All Terrain Vehicles.” Materials Today: Proceedings 59: 878–83.

[39] Viqaruddin, Mohod. 2016. “Review of Structural Optimization of Control Arm for Weight Reduction and Improved Performance”.

[40] Y. Peng, "Topological Optimization of Automobile’s Control Arm," *2022 IEEE Asia-Pacific Conference on Image Processing, Electronics and Computers (IPEC)*, Dalian, China, 2022, pp. 1610-1615

[41] Harzheim, L., Graf, G. 2006. A review of optimization of cast parts using topology optimization. Struct Multidisc Optim 31, 388–399.

[42] Ugale, Akshay N., Babaso N. Naik, and Abhinandan B. Admuthe. 2022. "Topology Optimization of the Double Wishbone Suspension System Components and Vibration Analysis." Journal of Automation and Automobile Engineering.

[43] Bhat, A., Gupta, V., Aulakh, S.S. and Elsen, R.S. 2023, "Generative design and analysis of a double-wishbone suspension assembly: a methodology for developing constraint oriented solutions for optimum material distribution", Journal of Engineering, Design and Technology, Vol. 21 No. 3, pp. 927-942.

[44] Pawar, Ashish R., Madhuri V. Bodke, and Aditya R. Wankhade. "Static Structural Analysis & Optimization of Concept Automotive A-Arm."

[45] “The Best Automotive Software Applications Used by Engineers.” 2023. Valispace. Accessed on June 25th, 2023. https://www.valispace.com/best-automotive-software-applications/.

[46] “Fusion 360 Help.” Help.autodesk.com. Accessed June 30th, 2023. https://help.autodesk.com/view/fusion360/ENU/?guid=GD-SPECIFY-MFG-METHOD.

[47] Davis, Andrea & Huxol, Andrea & Villmer, Franz-Josef & Scheideler, Eva. (2017). Deployment of Process Capability Analysis for Single-Part Production Production Engineering and Management Proceedings 7th International Conference, 2017, pp. 63-74.

[48] Consultancy. 2016. “3D Printing Market to Grow to 12.5 Billion by 2018.” April 25th, 2016.
https://www.consultancy.uk/news/11904/3d-printing-market-to-grow-to-125-billion-by-2018.

[49] Reliance Foundry. “Review of Ask a Metallurgist: A Brief Intro to Aluminum Grades”.
https://www.reliance-foundry.com/blog/grades-of-aluminum.

[50] “Null.” n.d. Materials UK. Accessed on March 23rd, 2023
https://www.thyssenkrupp-materials.co.uk/aerospace-grade-aluminum.

[51] He, Jeremy. “EN8 Carbon Steel, 080M40 BS 970 Specification.” Otai Special Steel.
https://www.astmsteel.com/product/en8-carbon-steel-080m40-bs-970/.

[52] Steel Express. “EN8 Engineering Steel | 080M40 | Steel Express.” Accessed March 24th, 2023.
https://www.steelexpress.co.uk/engineeringsteel/EN8.html.

[53] “EN8, EN8D, EN8M Steel.” 2009.
https://kvsteel.co.uk/steel/EN8.html.

[54] Smith Metal. “EN8 Engineering Steel | 080M40 Engineering Steel | Smiths Metal Centres Ltd.”
https://www.smithmetal.com/en8.htm.

[55] Saaj Steel Corporation. “EN47.” Accessed March 24th, 2023.
https://www.saajsteel.com/spring-steel-round-bar-manufacturers-and-suppliers-in-chennai/en47-spring-steel-bar-manufacturers-suppliers-in-chennai/.

[56] West Yorkshire Steel. “EN47 in Stock. On Time Delivery. UK ISO 9001 Supplier.” Accessed March 24th, 2023.
https://www.westyorkssteel.com/spring-steel/en47/.

[57] Dhand Steels. “EN 47 Spring Steel | Dhand Steels.” Bright Bars Manufacturer and Supplier in Ludhiana, Punjab, India. Accessed March 24th, 2023.
https://dhandsteels.com/en-47-spring-steel/.

[58] Furnival Steel. “EN47 Spring Steel.” Accessed March 24th, 2023.
https://www.furnivalsteel.co.uk/en47-spring-steel.

[59] Scribd. “En 47 | PDF | Steel | Heat Treating.” Accessed March 24th, 2023.

[60] Saaj Steel Corporation. “EN47.” Accessed March 24th, 2023. https://www.saajsteel.com/spring-steel-round-bar-manufacturers-and-suppliers-in-chennai/en47-spring-steel-bar-manufacturers-suppliers-in-chennai/.

[61] Ulbrich. “2000 Series Aluminum Alloys.” https://www.ulbrich.com/alloys/2000-series-aluminum-alloys/.

[62] Euralliage. “Alliages d’ Aluminium.” Accessed March 23rd, 2023. https://www.euralliage.com/alliage_english.htm.

[63] Abdel-Salam, Omar & Shoeib, Madiha & Elkelany, Hager. 2017. “Characterization of the hard anodizing layers formed on 2014-T3 Al alloy, in sulphuric acid electrolyte containing sodium lignin sulphonate”. Egyptian Journal of Petroleum. 27.

[64] Ulbrich. “5000 Series Aluminum Alloys.” Accessed March 24th, 2023. https://www.ulbrich.com/alloys/5000-series-aluminum-alloys/.

[65] Ulbrich. “6000 & 7000 Series Aluminum Alloys.” Accessed March 23rd, 2023. https://www.ulbrich.com/alloys/6000-7000-series-aluminum-alloys/?gclid=Cj0KCQjw8e-gBhD0ARIsAJiDsaUVz8-.

[66] Cara. 2021. “6000 Series Aluminum Alloys.” Taber Extrusions. https://taberextrusions.com/6000-series-aluminum-alloys/.

[67] “6000 Series Aluminum Alloys.” Accessed March 24th, 2023. https://www.jmhaluminum.com/newsclass_3/newsdetail_19.shtml.

[68] Ulbrich. “6000 & 7000 Series Aluminum Alloys.”. Accessed March 23rd, 2023. https://www.ulbrich.com/alloys/6000-7000-series-aluminum-alloys/?gclid=Cj0KCQjw8e-gBhD0ARIsAJiDsaUVz8-l96Di0AtrZoHSYI7a0KVgH7d5ITs53qYQNhfUg8ZzZrp0ZqUaAnlcEALw_wcB.

[69] Smith Metal. 2016. “7000 Series Aluminium Alloys | Smiths Metal Centres Ltd.” https://www.smithmetal.com/7000-series-aluminium-alloys.htm.

[70] Smith Metal. “7050 Aluminium Alloy | 7050 T7451.” https://www.smithmetal.com/7050.htm.

[71] Smith Metal. “7068 Aluminium | 7068 Aluminium Alloy | al 7068.” https://www.smithmetal.com/7068.htm.

[72] Smith Metal. 2016. “7075 Aluminium Alloy | Smiths Metal Centres Ltd.” https://www.smithmetal.com/7075.htm.

[73] Ansys GRANTA EduPack software, ANSYS, Inc. Cambridge, UK, 2022 (www.ansys.com/materials)

[74] “Factor of Safety.” 2023. SafetyCulture. Accessed April 6th, 2023. https://safetyculture.com/topics/factor-of-safety/.

[75] Engineering Toolbox. 2010. “Factors of Safety.” https://www.engineeringtoolbox.com/factors-safety-fos-d_1624.html.

[76] “What Is Factor of Safety (FoS)? - Definition from WhatIs.com.” https://www.techtarget.com/whatis/definition/factor-of-safety-FoS.

[77] Wilhite, Lindsey. 2018. “Factor of Safety: What Is It and Why Is It Important?” Onsite Safety. https://www.onsitesafety.com/safety-articles/what-is-the-factor-of-safety/.

APPENDIX

1 Technical drawing of initial Steering Knuckle and Control arm

